

Simon Kelley

*Department of Earth Sciences
The Open University
Milton Keynes MK7 6AA, United Kingdom
s.p.kelley@open.ac.uk*

INTRODUCTION — A BIT OF HISTORY

The aim of this chapter is to present the K-Ar and Ar-Ar dating techniques in the context of noble gas studies, since there are already several recent texts on K-Ar and Ar-Ar dating (Dickin 1995; McDougall and Harrison 1999). The focus of this section will be aspects of argon transport and storage in the crust, which affect K-Ar and Ar-Ar dating including Ar-loss from minerals by diffusion and Ar-gain by minerals or “excess argon.”

The K-Ar dating technique was one of the earliest isotope dating techniques, developed soon after the discovery of radioactive potassium, and provided an important adjunct to U-Pb and U-He dating techniques. The ease of measurement and ideal half-life (1250 million years; see Table 2 below), for dating geological events has made this the most popular of isotopic dating techniques. Aldrich and Nier (1948) first demonstrated that ^{40}Ar was the product of the decay of ^{40}K , and soon after K-Ar ages were being measured in several laboratories most often using an absolute method such as a McLeod gauge to measure argon concentrations. The first published K-Ar results by such a technique were those of Smits and Gentner (1950) who analyzed sylvite from the Buggingen Oligocene evaporite deposits, obtaining an age of 20 million years. Mass spectrometers, which simultaneously measured very small amounts of gas, and the isotope ratios necessary to make corrections for atmospheric contamination, quickly replaced manometric techniques. Crucially the use of static vacuum techniques, pioneered by John Reynolds at the University of California-Berkeley, meant that mass spectrometers were sufficiently sensitive to analyse the small amounts of gas released from common rocks and minerals. Although the earliest mass spectrometers were built ‘in house’, the introduction of the commercially available MS10 (Farrar et al. 1964), a small 180° metal mass spectrometer built for leak testing, made K-Ar dating generally available. Complete descriptions of early K-Ar development and techniques can be found in Schaeffer and Zähringer (1966) and Dalrymple and Lanphere (1969).

Although Thorbjorn Sigurgeirsson proposed the principles of Ar-Ar dating in an unpublished Icelandic laboratory report in 1962, he never succeeded in publishing or testing the idea. The Ar-Ar dating technique as it is practised today originated in the noble gas laboratory of John Reynolds in Berkeley, where Craig Merrihue and Grenville Turner were working on neutron irradiated meteorite samples using the I-Xe dating technique. Merrihue recognised that a ^{39}Ar signal seen in the chart recorder traces was the result of neutron irradiation and published the idea in an abstract (Merrihue 1965). The publication of Merrihue and Turner (1966) saw the birth of the Ar-Ar dating technique. Written by Turner after the untimely death of Merrihue, this paper unusually describes a fully formed isotope dating technique (compare this with the slow emergence of the full K-Ar technique), possibly because the Berkeley Laboratory had been recording the full traces of all noble gases for some time, allowing Merrihue and Turner rapid access to a considerable database of measurements. The advantage of the Ar-Ar technique is that potassium and argon are effectively measured simultaneously on the same aliquot of sample, providing greater internal precision and also the ability to analyse very small and

heterogeneous samples. Ar-Ar dating proved to be an ideal technique for dating meteorites because it made the best use of the extremely limited number of samples and also provided thermal histories. Indeed when lunar samples were returned from the Apollo 11 mission, Ar-Ar provided a crucial dating technique. Some samples were dated using K-Ar and yielded ages in the broad range 3 to 4 Ga, testifying to the antiquity of the lunar surface, although this much had been estimated from crater densities. In contrast, the Ar-Ar dating technique provided a wealth of precise ages and thermal histories. Using very small samples, Grenville Turner was able to unravel the crystallization histories, thermal histories during post-eruption heating and the cosmic ray exposure histories in a classic series of papers (Turner 1970b,c; 1971b, 1972). Turner applied quantitative diffusion concepts to stepwise argon release and recovered information from partially outgassed samples, establishing techniques and protocols that are still used to interpret stepwise heating Ar-Ar spectra today. This work and much of the early history of the Ar-Ar dating technique are set out in detail in McDougall and Harrison (1999).

Although this chapter describes both K-Ar and Ar-Ar techniques, it should be noted that K-Ar dating is now important in only limited situations including standardization (i.e., first principles dating of standards), dating fine grained clay samples, dating young basalts and obtaining dates in rapid turnaround times. Ar-Ar dating is now used in a very wide range of geological applications, dating samples as old as lunar basalts and primitive meteorites, and volcanic rocks erupted only 2000 years ago. Ar-Ar dating has been applied to many areas of Earth Sciences for dating igneous, metamorphic and sedimentary events. In recent years the introduction of laser techniques for single spot and laser heating analysis has widened the range of applications for Ar-Ar dating and the introduction of more sophisticated models for stepwise heating continue to provide ever more detailed thermal histories from K-feldspars.

THE K-AR AND AR-AR DATING METHODS

Introduction

Both K-Ar and Ar-Ar dating techniques are based upon the decay of a naturally occurring isotope of potassium, ^{40}K to an isotope of argon, ^{40}Ar (Fig. 1). The decay of ^{40}K is by a branching process; 10.48% of ^{40}K decays to ^{40}Ar by β^+ decay (Beckinsale and Gale 1969, also proposed gamma-less electron capture decay but this has never been verified), followed by γ decay to the ground state, and by electron capture direct to the ground state, and 89.52% decays to ^{40}Ca by β^- to the ground state (Fig. 1). ^{40}K - ^{40}Ca dating using the more common branch is also possible (e.g., Marshall and DePaolo 1982), but its application is generally restricted to old potassium-rich rocks since ^{40}Ca is the most abundant naturally occurring isotope (96.94%), making the small amounts of radiogenically produced ^{40}Ca very difficult to measure. Argon, in contrast, is a rare trace element and radiogenically produced ^{40}Ar generally exceeds the levels of trapped ^{40}Ar (although this is not always the case—see later). The naturally occurring isotopes of argon are measured by mass spectrometry for K-Ar dating (^{36}Ar , ^{38}Ar and ^{40}Ar). The $^{36}\text{Ar}/^{38}\text{Ar}$ ratio is almost constant (see Table 1), although cosmogenic ^{38}Ar can be detected in some Ca-rich samples (Renne et al. 2001). Absolute argon concentrations, required for the K-Ar technique, are measured as a ratio against a known amount of ^{38}Ar tracer gas. Mass spectrometry for Ar-Ar dating requires only isotope ratios between naturally occurring isotopes and also reactor produced isotopes ^{39}Ar and ^{37}Ar which have half lives of 269 years and 34.95 days respectively. As we shall see later, the irradiation procedure produces not only the radioactive isotopes but also small amounts of stable isotopes of argon, and it is thus important to measure all argon masses precisely by mass spectrometry in order to correct for neutron-induced interferences.

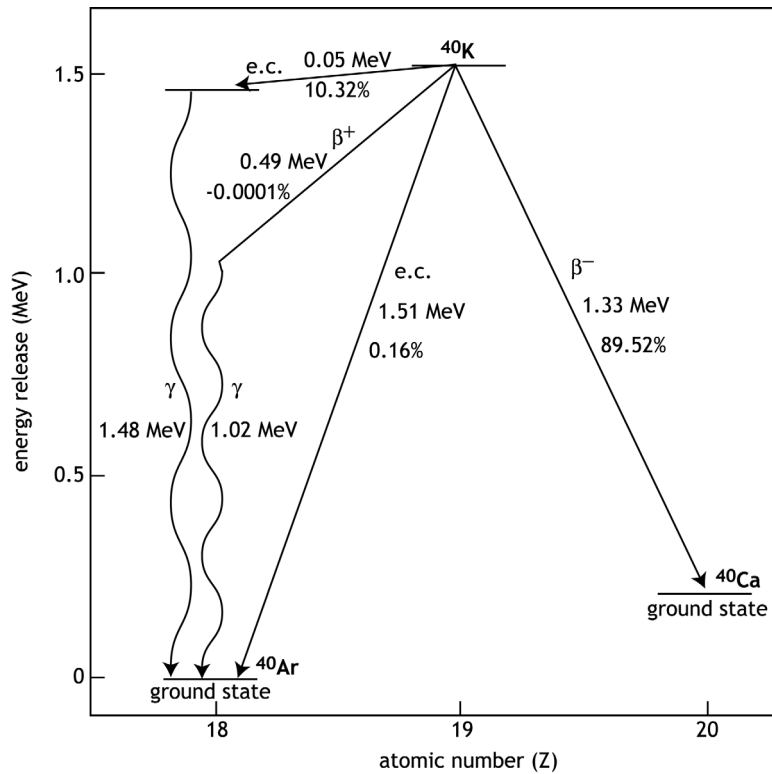


Figure 1. Branching diagram showing the decay scheme for ^{40}K , showing decay to ^{40}Ar and ^{40}Ca (after McDougall and Harrison 1999).

Table 1. Naturally occurring iso- topes of argon and potassium.

Isotope	Abundance (%)
^{40}Ar	99.600
^{38}Ar	0.632
^{36}Ar	0.336
^{39}K	93.2581
^{40}K	0.01167
^{41}K	6.7302

After Steiger and Jäger (1977).

The essential difference between K-Ar and Ar-Ar dating techniques lies in the measurement of potassium. In K-Ar dating, potassium is measured generally using flame photometry, atomic absorption spectroscopy, or isotope dilution and Ar isotope measurements are made on a separate aliquot of the mineral or rock sample. In Ar-Ar dating, as the name suggests, potassium is measured by the transmutation of ^{39}K to ^{39}Ar by neutron bombardment and the age calculated on the basis of the ratio of argon isotopes.

Assumptions

The “date” measured by both K-Ar and Ar-Ar techniques reflects the time since radiogenic argon produced by decay of ^{40}K , became trapped in the mineral or rock. This may be the “age” of the rock or the most recent cooling event and in some samples may even reflect an integrated cooling age for a range of sub-grains. However, like all isotope-dating techniques, there is a set of assumptions that must be valid if the number measured is to be interpreted as the age of a geological event:

1. The decay of the parent nuclide, potassium must be independent of its physical state. This is the standard assumption that must be valid for any isotope dating technique.
2. The $^{40}\text{K}/\text{K}$ ratio must be a constant at any given time (Table 1). Most recently

(Humayun and Clayton 1995a; Humayun and Clayton 1995b) measured a range of samples and found less than 0.05% variation in the $^{39}\text{K}/^{41}\text{K}$ ratio, even in samples where previous studies had measured some variation.

3. All radiogenic ^{40}Ar measured in the sample results from ^{40}K decay. The occasional presence of contaminating ^{40}Ar from various sources can make determining the actual radiogenic content difficult but these are not strictly speaking radiogenic argon (see below).
4. Corrections can be made for any non-radiogenic argon. This is a simple procedure in terrestrial samples where there is generally some contaminating argon from the atmosphere (0.934% argon), but with a constant $^{40}\text{Ar}/^{36}\text{Ar}$ ratio of 295.5 (Table 1). Such corrections are less simple in extra-terrestrial samples where the initial $^{40}\text{Ar}/^{36}\text{Ar}$ ratios are not constant, and are generally achieved using an isochron plot. Cosmogenic contributions are considered elsewhere in this volume (Wieler 2002; Niedermann 2002).
5. The sample, whether mineral or whole rock, must have remained a closed system since the event being dated. This includes gain or loss of either argon or potassium. This assumption is sometimes invalid, particularly in systems with complex geological and thermal histories. However, Ar-Ar stepwise heating and laser spot techniques can often be used to extract thermal history information from partially opened systems, taking advantage of the manner and extent of argon loss.

Table 2. Decay constants for K-Ar and Ar-Ar dating. After Steiger and Jäger (1977).

<i>Decay</i>	<i>Decay factor</i>	<i>Value</i>
$^{40}\text{K} \rightarrow ^{40}\text{Ca}$ by β^-	λ_{β^-}	$4.962 \times 10^{-10} \text{ a}^{-1}$
$^{40}\text{K} \rightarrow ^{40}\text{Ar}$ by electron capture and γ	λ_e	$0.572 \times 10^{-10} \text{ a}^{-1}$
$^{40}\text{K} \rightarrow ^{40}\text{Ar}$ by electron capture	λ'_e	$0.0088 \times 10^{-10} \text{ a}^{-1}$
combined value	$\lambda = \lambda_{\beta^-} + \lambda_{ec} + \lambda'_{ec}$	$5.543 \times 10^{-10} \text{ a}^{-1}$
	present day $^{40}\text{K}/\text{K}$	0.0001167

CALCULATING K-AR AND AR-AR AGES

The age equation for the K-Ar isotope system is:

$$t = \frac{1}{\lambda} \ln \left[1 + \frac{\lambda}{\lambda_e + \lambda'_e} \frac{^{40}\text{Ar}^*}{^{40}\text{K}} \right] \quad (1)$$

where t is the time since closure, λ is the total decay of ^{40}K , and $(\lambda_e + \lambda'_e)$ is the partial decay constant for ^{40}Ar (Begemann et al. 2001) (Table 2). $^{40}\text{Ar}^*/^{40}\text{K}$ is the ratio of radiogenic daughter product (shown conventionally as $^{40}\text{Ar}^*$ to distinguish it from atmospheric ^{40}Ar) to the parent ^{40}K . Since there is no common natural fractionation of potassium isotopes (Humayun and Clayton 1995a,b), the modern ratio of $^{40}\text{K}/\text{K}$ is a constant (Table 1), and thus measurement of potassium and argon concentrations together with isotope ratios of Ar, enable an age to be calculated.

The Ar-Ar technique, first described by Merrihue and Turner (1966), is based on the same decay scheme as K-Ar, but instead of measurement on a separate aliquot, potassium is measured by creating ^{39}Ar from ^{39}K by neutron bombardment in a nuclear reactor. The reaction induced is:



The ratio of ^{39}K to ^{40}K is effectively constant (see above) and thus the critical $^{40}\text{Ar}^*/^{40}\text{K}$

ratio is proportional to the ratio of the two argon isotopes $^{40}\text{Ar}/^{39}\text{Ar}$. Although ^{39}Ar is radioactive, decaying with a half-life of 269 years, this effect is small for the period between irradiation and analysis (generally less than 6 months) and is easily corrected for.

Mitchell (1968) showed that the number of ^{39}Ar atoms formed during irradiation can be described by the equation:

$$^{39}\text{Ar} = ^{39}\text{K} \Delta \int \varphi(\varepsilon)\sigma(\varepsilon)d(\varepsilon) \quad (3)$$

where ^{39}K is the number of atoms, Δ is the duration of the irradiation, $\varphi(\varepsilon)$ is the neutron flux density at energy ε , and $\sigma(\varepsilon)$ is the neutron capture cross section of ^{39}K for neutrons of energy ε for the neutron in/proton out reaction shown in Equation (2).

Rearranging Equation (1) in terms of $^{40}\text{Ar}^*$ yields:

$$^{40}\text{Ar}^* = ^{40}\text{K} \frac{\lambda_e + \lambda'_e}{\lambda} [(e^{\lambda t}) - 1] \quad (4)$$

Combining Equations (3) and (4) for a sample of age t yields:

$$\frac{^{40}\text{Ar}^*}{^{39}\text{Ar}} = \frac{^{40}\text{K}}{^{39}\text{K}} \frac{\lambda_e + \lambda'_e}{\lambda} \frac{1}{\Delta T} \frac{[(e^{\lambda t}) - 1]}{\int \varphi(\varepsilon)\sigma(\varepsilon)d(\varepsilon)} \quad (5)$$

This can be simplified by defining a dimensionless irradiation-related parameter, J , as follows:

$$J = \frac{^{39}\text{K}}{^{40}\text{K}} \frac{\lambda}{\lambda_e + \lambda'_e} \Delta T \int \varphi(\varepsilon)\sigma(\varepsilon)d(\varepsilon) \quad (6)$$

The J value is determined by using mineral standards of known age to monitor the neutron flux. Substituting Equation (6) into Equation (5) and rearranging, yields the Ar-Ar age equation:

$$t = \frac{1}{\lambda} \ln \left[1 + J \frac{^{40}\text{Ar}^*}{^{39}\text{Ar}} \right] \quad (7)$$

The ratio of the two isotopes of argon, naturally produced radiogenic ^{40}Ar and reactor-produced ^{39}Ar is thus proportional to the age of the sample. For terrestrial samples, the ^{40}Ar peak measured in the mass spectrometer most often has two components (neglecting the $^{40}\text{Ar}_K$ interference reaction), radiogenic and atmospheric. The $^{40}\text{Ar}/^{36}\text{Ar}$ ratio of the atmosphere was determined by IUGS convention as 295.5 (Table 1; Steiger and Jäger 1977), though Nier determined a value of 296 (Nier 1950). When the $^{40}\text{Ar}/^{36}\text{Ar}$ ratio of contaminating argon components is >295.5 , the extra argon is known as extraneous argon. The term extraneous argon includes both excess and inherited argon following the terminology of Dalrymple and Lanphere (1969) and McDougall and Harrison (1999). Excess argon is the component of argon incorporated into samples by processes other than *in situ* decay, generally from a fluid or melt at the grain boundary. Inherited argon results from the incorporation of older material in a sample, such as for example grains of sand caught up in an ignimbrite eruption. However, in the simple case, assuming that all the non-radiogenic argon is atmospheric, the daughter/parent ratio ($^{40}\text{Ar}^*/^{39}\text{Ar}$) can be determined from the equation:

$$^{40}\text{Ar}^*/^{39}\text{Ar} = [^{40}\text{Ar}^*/^{39}\text{Ar}]_m - 295.5 [^{36}\text{Ar}/^{39}\text{Ar}]_m \quad (8)$$

where subscript m denotes the measured ratio. This equation is always a simplification; in most terrestrial samples surface contamination ensures that some atmospheric argon is present, though fluids at depth rarely have atmospheric ratios (see below). However, in

extraterrestrial samples atmospheric argon is recognised as a modern contamination or the result of weathering. In this light, it might seem strange to assume that all contaminating argon in terrestrial samples has an atmospheric isotope ratio, given that many trap argon at depth, not in equilibrium with the atmosphere. This puzzle will be discussed in some detail in the later section on argon diffusion and solubility.

Sample irradiation for Ar-Ar dating induces not only Reaction (2) but also a series of interfering reactions caused by neutron bombardment of potassium, calcium, chlorine and argon. The complete series of interfering reactions is detailed in Table 3, but most have low production rates relative to the reaction in Equation (3) and can be ignored. The most important reactions are those involving calcium and potassium. The corrections are generally small, though they are critical for samples younger than 1 Ma when the interfering reactions producing ^{40}Ar from ^{40}K are important, and for samples with $\text{Ca}/\text{K} > 10$, when reactions producing ^{36}Ar and ^{39}Ar from isotopes of Ca become important. The magnitude of the interference from these reactions varies with the irradiation time and neutron flux energy spectrum. The range of measured interference factors for many of the world's reactors are listed in McDougall and Harrison (1999).

The $^{42}\text{Ca}(\text{n},\alpha)^{39}\text{Ar}$ and $^{40}\text{Ca}(\text{n},\alpha)^{36}\text{Ar}$ production ratios do not vary a great deal, because they are caused by fast neutrons and the energy spectrum of fast neutrons in most reactors is fairly similar. The far larger variation in the interference in the $^{40}\text{K}(\text{n},\text{p})^{40}\text{Ar}$ reaction is caused by its higher sensitivity to the ratio of fast to thermal neutrons in the reactor. This ratio varies between reactors and also between different irradiation positions within a reactor. In fact samples are often shielded with cadmium foil to reduce the thermal neutron flux and lower the efficiency of the $^{40}\text{K}(\text{n},\text{p})^{40}\text{Ar}$ reaction. The precise correction factors can be determined by irradiating pure salts of Ca and K (often CaF_2 , KCl and K_2SO_4). An additional correction must also be made for the decay of ^{37}Ar (produced by neutron bombardment of calcium) which has a half-life of 34.95 ± 0.08 days (Renne and Norman 2001). The short half-life of ^{37}Ar means that all Ca-rich samples must be analyzed within about 6 months of irradiation otherwise the precision determining the original ^{37}Ar concentrations may be affected, compromising the corrections to ^{36}Ar and ^{39}Ar for Ca irradiation.

Another factor affecting the accuracy of Ar-Ar dating is ^{39}Ar recoil. This effect is crucial when studying very fine scale argon distributions or fine grained minerals such as clays, but ^{39}Ar recoil from mineral surfaces can also affect high precision dating. Turner and Cadogan (1974), calculated the likely distances of ^{39}Ar recoil during irradiation to be a mean of $0.08 \mu\text{m}$, a study which was refined by Onstott et al. (1995) and measured directly by Villa (1997). The effects are most obviously detected in measurements of fine grained clays (e.g., Foland et al. 1983), but are commonly cited as a reason for variable ages produced from altered minerals (Lo and Onstott 1989), and basaltic rocks (e.g., Baksi 1994; Feraud and Courtillot 1994).

The Ar-Ar technique is able to achieve higher levels of internal precision than K-Ar dating since it does not depend upon separate absolute measurements but instead requires only the ratios of Ar isotopes and can achieve precision of better than 0.25%. However, external precision and accuracy are affected by the uncertainty in the age of mineral standards, as we will see in the following section. In order to achieve optimum precision in the mass spectrometric measurements, the neutron flux (which affects the magnitude of the J value) must be carefully selected. The flux must be sufficient for precise measurement of ^{39}Ar and a $^{40}\text{Ar}^*/^{39}\text{Ar}$ ratio within the dynamic range of the mass spectrometer (generally less than 100 for good precision). Further, at higher flux levels the interfering reactions on Ca and K also become more important, degrading the precision and accuracy with which the $^{40}\text{Ar}^*/^{39}\text{Ar}$ ratio may be determined. Therefore, for

Table 3. Interfering reactions on Ca, K, Ar and Cl.
Important interfering reactions are shown in bold type. The main ^{39}Ar -producing reaction is shown with a single border.

Argon isotope	Ca	K	Ar	Cl
^{36}Ar	$^{40}\text{Ca}(\text{n},\text{n}\alpha)^{36}\text{Ar}$			$^{35}\text{Cl}(\text{n},\gamma)^{36}\text{Cl} \rightarrow \beta^- \rightarrow ^{36}\text{Ar}$
^{37}Ar	$^{40}\text{Ca}(\text{n},\alpha)^{37}\text{Ar}$	$^{39}\text{K}(\text{n},\text{nd})^{37}\text{Ar}$	$^{36}\text{Ar}(\text{n},\gamma)^{37}\text{Ar}$	
^{38}Ar	$^{42}\text{Ca}(\text{n},\text{n}\alpha)^{38}\text{Ar}$	$^{39}\text{K}(\text{n},\text{d})^{38}\text{Ar}$	$^{40}\text{Ar}(\text{n},\text{nd})^{38}\text{Cl} \rightarrow \beta^- \rightarrow ^{38}\text{Ar}$	$^{37}\text{Cl}(\text{n},\gamma)^{38}\text{Cl} \rightarrow \beta^- \rightarrow ^{38}\text{Ar}$
^{39}Ar	$^{42}\text{Ca}(\text{n},\alpha)^{39}\text{Ar}$	$^{41}\text{K}(\text{n},\alpha)^{38}\text{Cl} \rightarrow \beta^- \rightarrow ^{38}\text{Ar}$	$^{39}\text{K}(\text{n},\text{p})^{39}\text{Ar}$	$^{38}\text{Ar}(\text{n},\gamma)^{39}\text{Ar}$
	$^{43}\text{Ca}(\text{n},\text{n}\alpha)^{39}\text{Ar}$	$^{40}\text{K}(\text{n},\text{d})^{39}\text{Ar}$	$^{40}\text{Ar}(\text{n},\text{d})^{39}\text{Cl} \rightarrow \beta^- \rightarrow ^{39}\text{Ar}$	
^{40}Ar	$^{43}\text{Ca}(\text{n},\alpha)^{40}\text{Ar}$	$^{40}\text{K}(\text{n},\text{p})^{40}\text{Ar}$		
	$^{44}\text{Ca}(\text{n},\text{n}\alpha)^{40}\text{Ar}$	$^{41}\text{K}(\text{n},\text{d})^{40}\text{Ar}$		

The terminology (a,b) used here refers to nuclear reactions taking place during irradiation where a is the incident particle and b is the resulting emission. The terms are n=neutron, p = proton, d = deuteron, α =and alpha particle, γ = a gamma particle and β^- = a positron.

each sample there is an optimum flux level and given that many samples are irradiated together, each package sent for irradiation is a compromise. Turner (1971a) calculated the fields for optimum J value, and correspondingly integrated neutron flux, which were upgraded by McDougall and Harrison (1999) in the light of higher sensitivity, higher resolution mass spectrometers (Fig. 2).

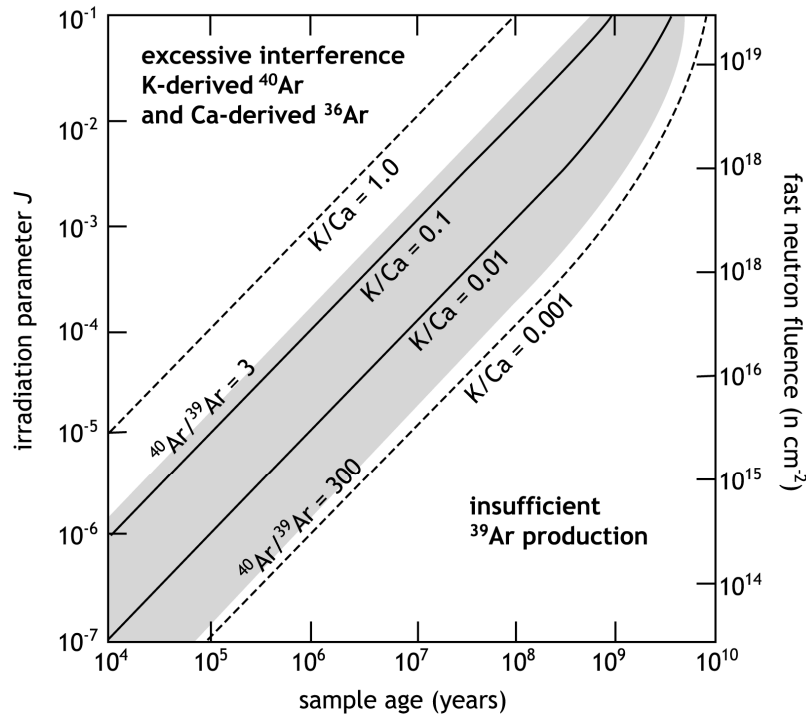


Figure 2. A Figure for optimizing irradiation parameters, taking account of age and Ca/K. The irradiation parameter is plotted against Age (Ma) and zones of optimum irradiation level are highlighted (after McDougall and Harrison 1999; Turner 1971a).

The availability of five argon isotopes provided by the Ar-Ar technique facilitates isotope correlation plots, the most common of which is the three isotope plot $^{36}\text{Ar}/^{40}\text{Ar}$ vs. $^{39}\text{Ar}/^{40}\text{Ar}$ (Fig. 3). Samples containing a mixture of radiogenic and atmospheric Ar plot along a line with negative slope between the $^{39}\text{Ar}/^{40}\text{Ar}$ ratio representing the age and the atmospheric $^{36}\text{Ar}/^{40}\text{Ar}$ ratio of 0.003384 (= 1/295.5) (Fig. 3a). The correlation plot also allows Ar-Ar ages to be calculated for samples with contamination other than modern air, since the age can equally be determined from lines passing through the $^{36}\text{Ar}/^{40}\text{Ar}$ axis at values other than the atmospheric ratio (Fig. 3b). However, a mixture of contaminating phases with more than one isotope composition in a sample results in a scatter of points not defining a line, and no age can be calculated. In many cases atmospheric ‘blank’ argon released from furnaces during heating is the only detected contaminating argon component. In cases where the contaminating argon is not homogeneous, physical techniques such as stepped heating, *in vacuo* crushing and laser spot dating have been used to separate components (see below).

The values of constants and estimation of errors

As the internal precision of Ar-Ar ages has improved over the years, the following have been the focus of debate:

1. The commonly accepted values for the K decay constants (Steiger and Jäger 1977)
2. The inter-laboratory and inter-standard calibration of Ar-Ar ages.

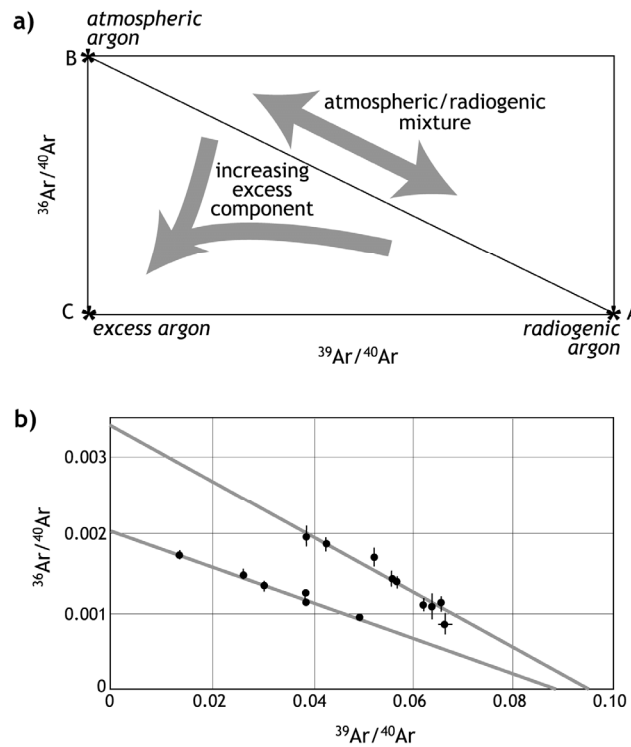


Figure 3. (a) An argon isotope correlation diagram, showing a correlation between atmospheric and radiogenic argon components which form an isochron. Any pure ^{40}Ar component would lie at the origin and thus any excess argon component tends to pull the point B towards the origin. (b) Two samples of amphibole analyzed by laser spot technique. The upper line intercepts within errors of atmospheric argon, the lower line yields a very similar age yet intercepts at a much lower $^{36}\text{Ar}/^{40}\text{Ar}$ ratio and contains excess argon.

K-Ar can be regarded as an absolute dating technique, dependent only on the value of the decay constant, and calibration of ^{38}Ar spike. However, all Ar-Ar ages are derived relative to the age of mineral standards, which are irradiated at the same time as the sample. The external precision of Ar-Ar ages is thus limited by the external precision of the age of the mineral standard as determined by the K-Ar method. The most widely used international standards are the hornblendes Hb3gr and MMHb1; biotites GA1550, GHC-305 and B4B, muscovite B4M, and sanidines from the Fish Canyon Tuff, Taylor Creek and Alder Creek (widely accepted ages for these standards are found in McDougall and Harrison 1999). Many other pure mineral samples are used as internal standards and several have been proposed as international standards but are not mentioned here since they are not in wide use. The advantage of using mineral standards is that they are freely available but since they are natural, series errors can be introduced if the various standards are not inter-calibrated. This has been an area of particular controversy in recent years, somewhat masking the improvements in internal precision. Fish Canyon Tuff is a prime example of the problems that are faced by those attempting to achieve accurate, and high precision Ar-Ar ages. Fish Canyon sanidine was proposed as an international standard by Cebula et al. (1986), who reported an age of 27.79 Ma but this was relative to another standard, MMHb1 with an age of 518.9 Ma (Alexander et al. 1978). When the age of the MMHb1 was revised to 520.4 Ma (Samson and Alexander 1987), the age of Fish Canyon sanidine became 27.84 Ma, though some workers used a value of 27.55 Ma, based on a different value for the age of MMHb1. In 1994, Renne et al. determined the age of Fish Canyon sanidine to be 28.03 Ma, an age later confirmed by

cross calibration (Renne et al. 1998b) with biotite standard GA1550. However, subsequent to 1994, many workers continued to use the value 27.84 Ma possibly because this yielded ages in agreement with the spline-fitted magneto-stratigraphic timescale, and in particular, the Cretaceous/Tertiary boundary of 65.0 Ma. Using the value recommended by Renne et al. (1998b) yields an age of 65.4 Ma for tektites from the K/T boundary. In addition, Lanphere and Baadsgaard (2001), maintain that a value of 27.51 Ma is the best age for Fish Canyon sanidine, based on Rb/Sr and U/Pb dates on Fish Canyon Tuff. The problem with this approach is that it requires cross calibration between dating methods, something that is even more fraught with problems. The decay constant of ^{87}Rb is no better constrained than ^{40}K (see below) and meteorite cross calibrations indicate ages may be as much as 2% too low (Renne 2000). In addition, the 27.52 ± 0.09 Ma bulk U/Pb age of Lanphere and Baadsgaard (2001) differs strongly from the U/Pb age of 28.476 ± 0.064 Ma obtained by Schmitz and Bowring (2001) on single grain and small multi-grain fractions of zircon, which confirmed an earlier determination of 28.41 ± 0.05 Ma by Oberli et al. (1990).

The work to improve the inter-calibration of standards has been accompanied by parallel discussions of the accuracy and precision of accepted decay constants of several important parent isotopes including ^{40}K (e.g., Begemann et al. 2001). It is notable that the decay constant quoted in most of the physical sciences literature is not the same as the one generally accepted for K-Ar and Ar-Ar dating. In 1977, based mostly on work by Beckinsale and Gale (1969) and Garner et al. (1975), Steiger and Jäger (1977) recommended the use of the decay constants in Table 2. However, Endt and Van der Leun (1973) later compiled the same data as Beckinsale and Gale (1969) to produce different results mainly by different selection criteria and statistical techniques. In a recent summary of ^{40}K decay constants, Audi et al. (1997) report a total decay constant of $5.428 \times 10^{-10} \text{ a}^{-1}$, as previously cited in the nuclear physics literature, a branching ratio of 89.28% and $^{40}\text{K}/\text{K} = 1.17 \times 10^{-4}$. Min et al. (2000) showed that a better correlation could be achieved between Ar-Ar and U-Pb ages using the decay constants of Endt and Van der Leun (1973) together with modern physical constants resulting in a total decay constant of $5.463 \pm 0.054 \times 10^{-10} \text{ a}^{-1}$ which corresponds to a half-life of 1269 ± 13 Ma. Renne (2000) further demonstrated that in one of the oldest rapidly cooled meteorites, called Acapulco, nuclear physics decay constants (Audi et al. 1997) produced Ar-Ar ages within errors of U-Pb ages, in line with the petrologic interpretation of these samples as rapidly cooled, whereas the existing Ar-Ar ages indicated slow cooling. Note that the interpretation of this important result is controversial (Trieloff et al. 2001; Renne 2001) and final resolution may await a more complete characterization of the thermal history of the Acapulco meteorite. (UTh)/He studies of Acapulco phosphates (Min et al. 2000) appear to validate the rapid cooling which supports the Audi et al. (1997) constants, particularly for the β^- decay (Min et al. 2001).

Reading this section may leave those new to K-Ar and Ar-Ar dating bemused by the current controversy over decay constants and the inter-calibration of standards in such a mature isotope dating technique. It must be emphasised that this controversy has arisen recently as the precision on age determinations has improved, and attempts are made to correlate with U-Pb ages, where decay constants are better constrained. Ages in the literature other than those cited above are still calculated using the decay constants recommended by Steiger and Jäger (1977), and Renne et al. (1998b) represents the most precise inter-calibration of standards combined with a precise K-Ar date on the GA1550 biotite standard using isotope dilution for the K analysis.

Analytical errors on the Ar-Ar age have generally been calculated using the simple error propagation of Dalrymple et al. (1981):

$$\sigma_t^2 \approx \frac{J^2 \sigma_R^2 + F^2 \sigma_J^2}{\lambda^2 (1 + FJ)^2} \quad (9)$$

where σ_t is the error on the age, J is the value from Equation (6), F is the $^{40}\text{Ar}^*/^{39}\text{Ar}$ ratio, λ is the combined decay constant, σ_R is the error on the $^{40}\text{Ar}^*/^{39}\text{Ar}$ ratio and σ_J is the error on the J value. A more complete numerical error analysis is given by Scaillet (2000). Errors on the age generally include the error in determining the J value, but not the external errors on determining the K-Ar age of the standard (e.g., GA1550) used to determine the neutron flux or the decay constants. However, when comparing Ar-Ar ages with ages determined by other isotope techniques such as U-Pb, these errors must be considered, something that is particularly important in dating short lived events such as terrestrial meteorite impacts or flood basalts. Renne et al. (1998a) present discussion of this problem and equations for calculating full external errors and appropriate errors when ages for samples measured against two different standards where those standards have been inter-calibrated.

ARGON DIFFUSION AND SOLUBILITY

K-Ar and Ar-Ar dating are isotope dating techniques, not isotope tracer techniques, but the trace element chemistry of argon plays an integral role in the assumptions and interpretation of K-Ar and Ar-Ar data. The use of the Ar-Ar dating technique to investigate cooling histories and understand extraneous argon are premised on an understanding of argon diffusion rates and argon solubility in hydrous fluids, melts and minerals. Below we will see how diffusion data provide the link between K-Ar or Ar-Ar age and the thermal history of the sample being investigated. We will also see how the assumption that all radiogenic daughter product ($^{40}\text{Ar}^*$) in a mineral results from the decay of ^{40}K is commonly contravened. In order to understand how this can happen, we need to consider partition and solubility of argon in fluid, melts and minerals.

Argon diffusion (and its use to determine thermal histories)

A full exposition of diffusion theory and diffusion mechanisms is beyond the scope of this chapter but the reader is referred to McDougall and Harrison (1999). Many observations show that argon diffusion rates in natural and laboratory experiments follow an Arrhenius relationship. There are however, important departures where fast track diffusion dominates in nature (Kramar et al. 2001; Reddy et al. 2001b) and laboratory analysis of hydrous minerals (Gaber et al. 1988; Lee 1993; Lo et al. 2000). Even in natural cases which might earlier have been identified as volume diffusion effects, careful compositional control shows that phase mixing can mimic argon loss profiles (e.g., Onstott and Peacock 1987; Wartho 1995). In such cases the data can not easily be inverted to produce thermal histories.

Having considered cases in which lattice or 'volume' diffusion does not explain the data, it should be noted that lattice diffusion seems to dominate many natural systems, in argon and other noble gases (cf. Farley 2002, this volume). Lattice diffusion follows a second order diffusion mechanism (McDougall and Harrison 1999) with an Arrhenius relationship given by the equation:

$$D = D_0 e^{\left(\frac{-E}{RT}\right)} \quad (10)$$

where D is the diffusion coefficient (m^2s^{-1}), D_0 is the pre-exponential factor (the theoretical diffusion constant at infinite temperature or a measure of 'conduction' in the mineral), E is the activation energy (J), R is the gas constant ($\text{J K}^{-1} \text{mol}^{-1}$) and T is temperature (K). This logarithmic relationship between diffusion rate and temperature means that at high temperatures, argon can diffuse through a mineral lattice and escape

into the grain boundary network much faster than it is produced by decay of ^{40}K . At low temperatures, diffusion rates are so slow that the daughter atoms are quantitatively retained in the mineral lattice (Fig. 4). There is also a temperature range of partial retention similar to the helium partial retention zone (HePRZ) of (U-Th)/He dating (Farley 2002, this volume), though this is generally quite narrow and represents a small length of time relative to the age of the sample. However the partial retention zone may become significant in slowly cooled metamorphic rocks (Dodson 1986; Lister and Baldwin 1996; Wheeler 1996). In early work, K-Ar ages of minerals such as biotite and muscovite were regarded as recording instantaneous closing temperatures and thus times in the cooling thermal history of the rock and closure temperatures were largely qualitative (e.g., Purdy and Jäger 1976), but Dodson (1973), provided an important advance by quantifying the closure temperature effect. By making a simplifying assumption, Dodson, showed that the closure temperature of a mineral could be described by the equation:

$$\frac{E}{RT_c} = \ln\left(\frac{A R T_c^2 D_0 / r^2}{E dT / dt}\right) \quad (11)$$

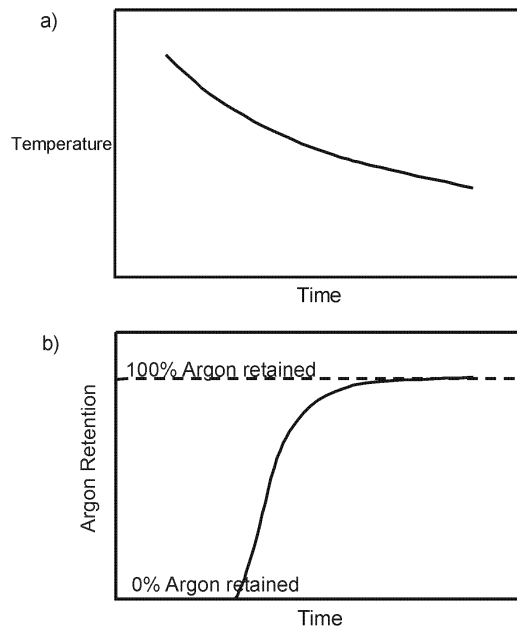


Figure 4. (a) A Temperature-time (Tt) curve for a cooling metamorphic terrain, in which the cooling rate is linear in $1/T$. (b) Although the cooling rate changes slowly, argon retention within a mineral, following the Tt path changes rapidly between rapid exchange to the grain boundary and no exchange. This sudden flip from open to closed gives rise to the closure temperature concept.

where E and D_0 are the activation energy and pre-exponential factor for argon diffusion, T_c is the closure temperature, R is the gas constant, r is the effective grain radius for argon diffusion (see discussion of diffusion domains below), dT/dt is the cooling rate at closure and A is a geometrical factor describing the variation of diffusion in the mineral ($A = 55$ for spherical geometry or equal diffusion in all three dimensions, $A = 27$ for cylindrical or diffusion dominantly in only two dimensions, and $A = 8.7$ for planar or dominantly one dimensional diffusion). The main simplifying assumption made by Dodson (1973) in order to produce this simple equation is that the cooling path of the rocks is linear in $1/T$. Although metamorphic cooling is commonly not linear in $1/T$, the

results are quite robust unless rocks are cooling very slowly. At cooling rates slower than around 5°C per million years, inner zones of grains close significantly earlier than the outer zones, leading to a closure temperature profile within the grain. Dodson (1986) took account of this slow cooling effect by the addition of an expression for the closure temperature as a function of position within the crystal. The function is tabulated in McDougall and Harrison (1999) and still suitable for rapid hand calculation. In more complex cases the diffusion equations can be solved numerically by finite difference, and programs such as DIFFARG (Wheeler 1996) allow the user to input any thermal history, limited only by the power of the computer. DIFFARG is suitable for calculations on single grains, but Lovera et al. (1997) have provided a technique for analysing multiple sub-grains or 'domains' by modeling ^{39}Ar release during laboratory experiments (see below).

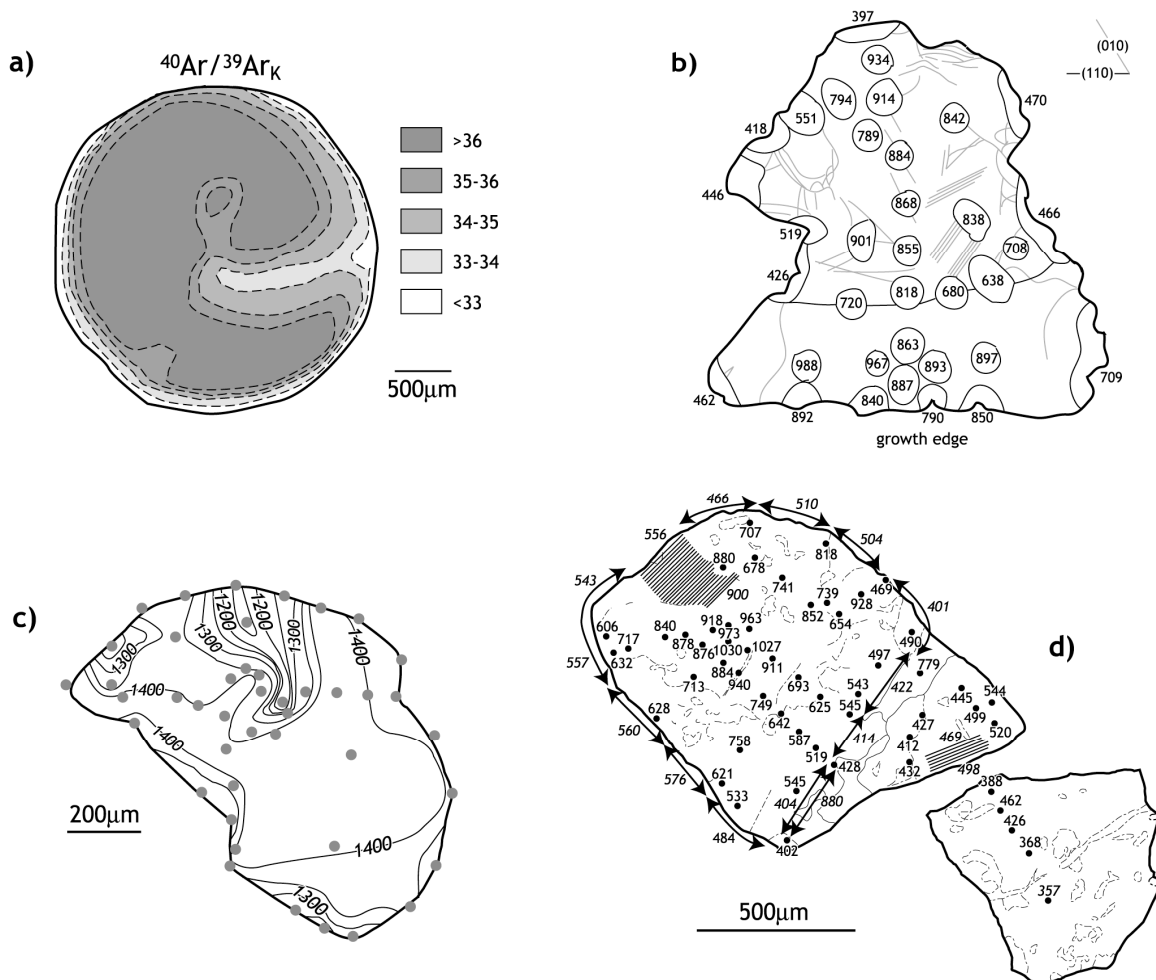


Figure 5. Laser profiles showing the effects of cracks and defects in minerals. (a) Biotite in an argon loss experiment, showing an indentation in the age contours resulting from a crack (Onstott et al. 1991). (b) Muscovite exhibiting young ages along an obvious fracture, shown left to right just below the center of the grain (Hames and Cheney 1997). (c) Biotite from a slowly cooled terrain again showing an indentation resulting from a crack (Hodges et al. 1994). (d) K-feldspar from a deformed sandstone, note that old ages are preserved in the center of this boudinaged grain but close to the boudin角度 and in the smaller fragment, only younger ages were measured (Reddy et al. 2001).

The discussion above considered only simple whole grain or sub-grain diffusion when lattice diffusion was the transporting mechanism. In recent years, the advent of laser analysis has demonstrated just how variable the actual within grain patterns can be (Fig. 5) (e.g., Hodges et al. 1994; Kelley and Turner 1991; Kramar et al. 2001; Lee et al.

1990; Phillips and Onstott 1988; Scaillet et al. 1990; Villa et al. 1996). Even before laser analysis had illustrated the patterns produced, bulk mineral analysis had shown that the relationship between grain size and argon loss broke down at larger grain sizes. Both natural (Layer et al. 1989; Wright et al. 1991) and laboratory (Grove and Harrison 1996) bulk heating experiments showed that the closure temperature did not increase as biotite grain size increased beyond around 150 μm , other bulk stepwise heating work determined effective radii up to 340 μm (Copeland et al. 1987), and yet age gradients have been measured in even larger grains (Hames and Cheney 1997). It seems likely that the effective diffusion radii are actually the result of variable cracking and defect density of the mica (Kramar et al. 2001; Mulch et al. 2001), particularly biotite which is the physically weaker of the two most commonly analyzed micas (Dahl 1996). Muscovite grains seem to retain metamorphic cooling age gradients even after erosion, transport and deposition in later sediments (e.g., Sherlock 2001).

Lee (1995) has proposed a model for fast-track diffusion to explain the effects of combined lattice diffusion and diffusion along fast diffusion pathways through the lattice such as defects. Lee proposed that the combined diffusion could be modeled as two parallel diffusion mechanisms with argon atoms partitioning between the two. The mathematical model produces realistic release patterns, but does not currently take account of the distances between fast track pathways and the time taken for atoms to reach one (cf. Arnaud and Kelley 1995). Future development of the fast track model may provide very fruitful avenues for research.

Argon solubility (and the causes of extraneous argon)

One of the fundamental assumptions of K-Ar dating (assumption 3, above) is that after correcting for atmospheric argon, all ^{40}Ar in the sample is the result of the *in situ* decay of ^{40}K , an assumption which is not always valid. However, the amounts of extraneous argon (see earlier definition) are small and generally remain undetected. Perhaps the best-known examples that contravene this assumption are the glassy rims to MORB basalts which retain significant quantities of argon derived from the upper mantle (Graham 2002, this volume). The solubility of noble gases in hydrous fluids and silicate melts have been studied extensively (Carroll and Draper 1994) but the data on mineral solubility and thus mineral fluid partition coefficients are less well known. Only in recent times have techniques been developed which can address the very low concentrations of noble gases in mineral lattices (e.g., Brooker et al. 1998; Chamorro et al. 2002; Wartho et al. 1999). The data which do exist imply very low partition coefficients between minerals and hydrous fluids and between minerals and melts. This explains how assumption 3 (above) can sometimes be invalidated and yet the dating technique still yields accurate, though often less precise, ages (Kelley 2002).

Early reports of excess argon covered the whole range of minerals and rocks (e.g., Dalrymple and Moore 1968; Damon and Kulp 1958; Livingston et al. 1967; Lovering and Richards 1964; Pearson et al. 1966) and most importantly, fluid inclusions (Rama et al. 1965). The step heating technique has been quite successful in discriminating against low concentrations of homogeneously distributed excess argon (e.g., Renne et al. 1997) which can be plotted on an isochron diagram (e.g., Heizler and Harrison 1988; Roddick 1978). In fact many published Ar-Ar ages contain small amounts of excess argon reflected in an initial $^{40}\text{Ar}/^{36}\text{Ar}$ ratio that is within a few percent of the atmospheric ratio. Such determinations yield precise results when the ratio of the contaminating component is close to that of atmospheric argon. However, as the ratio of the contaminant increases and the small ^{36}Ar peak becomes more difficult to measure, and the possibility of obtaining a precise age is quickly compromised. In extreme cases, excess argon may be undetected (e.g., Arnaud and Kelley 1995; Foland 1983; Pankhurst et al. 1973; Sherlock and Arnaud

1999). Further, the initial ratio correction only works when the isotope ratio within the samples is homogeneous, in cases of heterogeneous excess argon, a spread of data makes precise age determination impossible (e.g., Cumbest et al. 1994; Pickles et al. 1997).

The development of new analytical techniques for Ar-Ar dating has led to several advances in our understanding of excess argon. Ar-Ar stepped heating provides a physical technique to separate and analyse phases within individual samples as a result of their different breakdown temperatures (e.g., Belluso et al. 2000). Stepwise heating also produces decrepitation of fluid inclusions at low temperatures resulting in the high initial ages commonly observed in release spectra. Stepwise heating has also demonstrated excess argon diffusion into grain boundaries (Harrison and McDougall 1981). One feature of excess argon commonly associated with low potassium rocks and minerals such as plagioclase, amphibole and clinopyroxene is the saddle or 'U'-shaped Ar-Ar stepped heating release spectrum (Harrison and McDougall 1981; Lanphere and Dalrymple 1976; Wartho et al. 1996) (Fig. 6). Several explanations have been offered for this release pattern, first described by Dalrymple et al. (1975) and Lanphere and Dalrymple (1976) in samples from dykes intruding Pre-Cambrian rocks in Liberia. The initial Ar release yields old apparent ages, which decrease with progressive ^{39}Ar release, approaching the true age of the sample, and finally returning to older ages towards the end of argon release. Although arguments have been made for excess argon incorporation via special diffusion mechanisms such as anion diffusion (Harrison and McDougall 1981), recent data seem to demonstrate that the most likely candidates are fluid inclusions, released at low temperature, and melt or solid inclusions, released at high temperature during mineral breakdown (Boven et al. 2001; Esser et al. 1997) (Fig. 7).

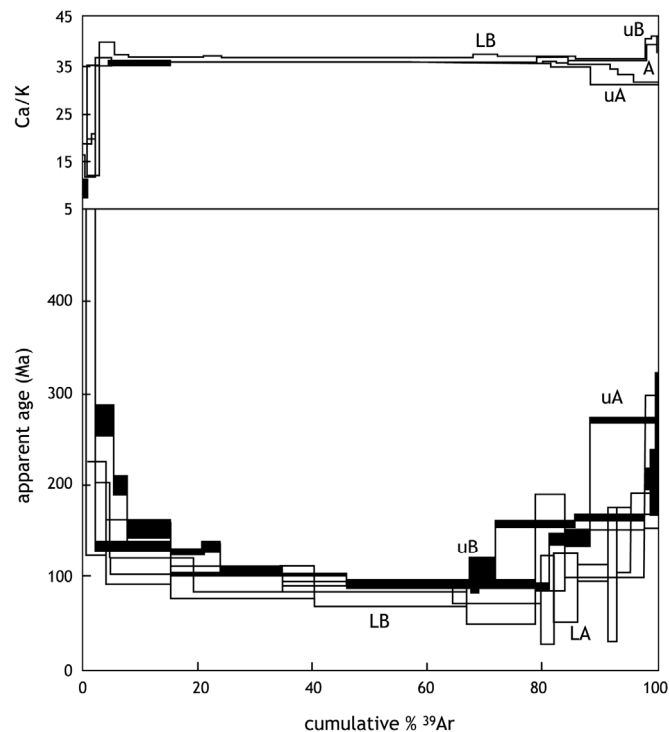


Figure 6. Excess argon in amphibole producing 'U' or 'saddle' shaped release spectrum. Dark spectra are original grains, light spectra are the same samples after acid leaching which reduced the excess argon component at both low and high ends of the release (Wartho et al. 1996).

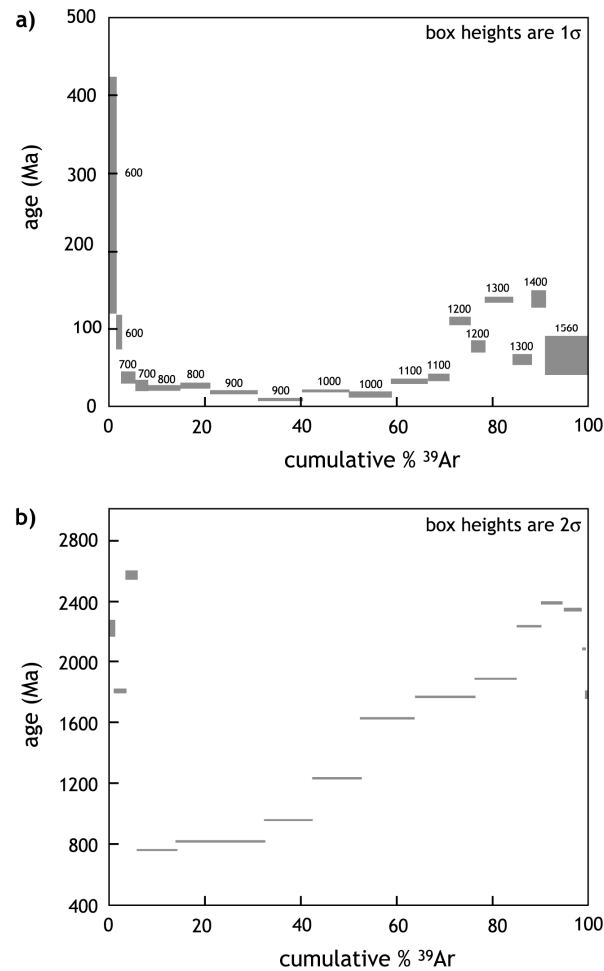


Figure 7. Saddle shaped spectra in plagioclase caused by excess argon dissolved in inclusions. (a) A zero age volcanic plagioclase with high melt inclusion content. (Esser et al. 1997). (b) A plutonic plagioclase showing a complex saddle shaped release pattern, probably the result of argon release from mixed phases (Boven et al. 2001).

Similar patterns have been seen in K-feldspars and these also probably relate to the interplay of fluid inclusion decrepitation at low temperature and excess argon in large sub-grains released at high temperature (Foster et al. 1990; Harrison et al. 1994; Zeitler and FitzGerald 1986).

In vacuo crushing has also been used to study the close correspondence between excess argon and saline crustal fluids trapped in fluid inclusions in quartz (Kelley et al. 1986; Turner and Bannion 1992; Turner et al. 1993) and K-feldspar (Burgess et al. 1992; Harrison et al. 1993, 1994; Turner and Bannion 1992). Finally, *in situ* laser spot extraction techniques have provided a method of investigating excess argon distributions within minerals, demonstrating close correlation between excess argon, and composition signatures inherited from the protolith in ultra-high-pressure UHP terrains (e.g., Giorgis et al. 2000; Sherlock and Kelley 2002), and demonstrating diffusion of excess argon through the mineral lattice (Fig. 8) (e.g., Lee et al. 1990; Pickles et al. 1997; Reddy et al. 1996).

Excess argon is most commonly found in metamorphic rocks, and is less common in volcanic systems where outgassing to the atmosphere provides a release mechanism. Excess argon is also particularly common in hydrothermal systems associated with large

granite intrusions (Kelley et al. 1986; Kendrick et al. 2001a,b; Turner et al. 1993), shear zones in ancient metamorphic terrains (Allen and Stubbs 1982; Smith et al. 1994; Vance et al. 1998), contact metamorphic aureoles (Harrison and McDougall 1980) and high and ultra-high-pressure metamorphic rocks (Arnaud and Kelley 1995; Inger et al. 1996; Li et al. 1994; Ruffet et al. 1997; Scaillet 1996; Scaillet et al. 1990, 1992; Sherlock et al. 1999; Sherlock and Kelley 2002).

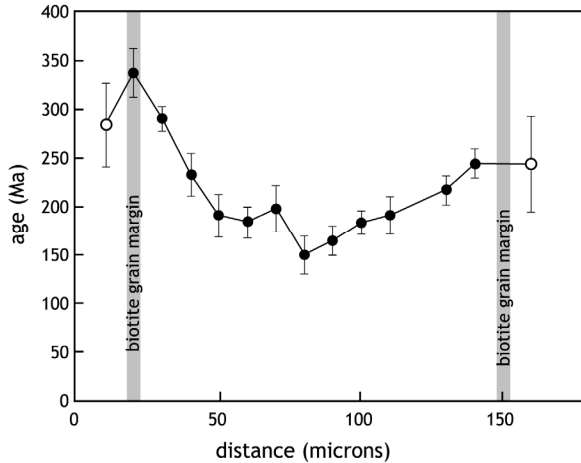
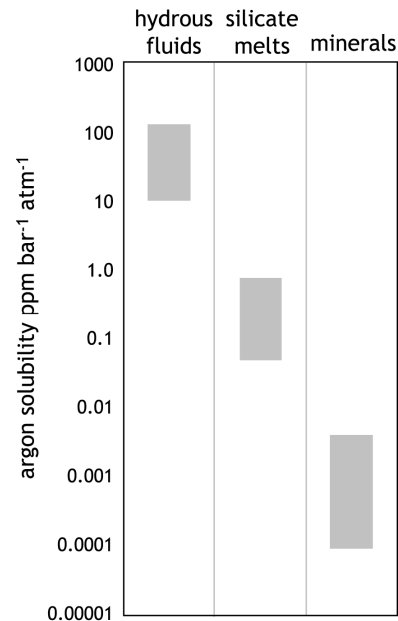


Figure 8. Excess argon diffusing into a biotite grain from the Seconda Zona Diorito Kinzigitica (IIDK) in the western Alps, the true cooling age of the biotites samples is around 40 Ma (from Pickles et al. 1997).

Figure 9. Comparison diagram of solubilities for hydrous fluids, melts and minerals based on data in Kelley (2002).



The importance of argon geochemistry is demonstrated clearly in Figure 9, which shows that argon is a highly incompatible trace element, strongly favoring partition from minerals into grain boundary fluids in metamorphic rocks, or from crystals into melts or melts into bubbles in magmatic systems, leaving minerals as the most highly depleted part of any system. Small amounts of excess argon may often be present but the concentrations are so low as to be masked by the larger radiogenic component. The corollary to this hypothesis is that more cases of excess argon are detected in low potassium minerals and the excess Ar is very often present in quartz (e.g., Kelley et al. 1986; Kendrick et al. 2001b; Rama et al. 1965; Turner and Bannon 1992; Vance et al. 1998). The highly incompatible nature of the argon in solid/melt and solid/fluid systems makes the fluids and melts effectively “infinite reservoirs” for radiogenic argon in these systems. More importantly however, the fact that some experimental data are available means that it is possible to model simple systems and define the limits of K-Ar and Ar-Ar dating. Although mineral data are sparse, reliable data now exist for olivine, phlogopite, clinopyroxene and K-feldspar (Brooker et al. 1998; Roselieb et al. 1999; Wartho et al.

1999). Emerging work on quartz, plagioclase, leucite and other minerals may add to this database (Roselieb et al. 1999; Wartho et al. unpublished data). In the following sections we will explore how the data for K-feldspar can be used to explore how natural systems might work.

Excess argon has been detected in both fluid-rich (open system) environments such as shear zones or hydrothermal systems and in fluid-poor (closed system) environments such as granulites or high-pressure metamorphic rocks. In fluid-rich environments, a fluid with a high concentration of excess argon is in contact with minerals above their closure temperature, and significant quantities of excess argon partition into the minerals, or just as likely, become incorporated as fluid inclusions (e.g., Cumbest et al. 1994; Kendrick et al. 2001a,b). In fluid-poor environments such as dry granulites or high- and ultra-high-pressure metamorphic rocks, fluids may only be present as transient phases in restricted zones. In such rocks, fluids do not travel significant distances (Philippot and Rumble 2000) and thus transport of argon along the grain boundaries might be as little as a few centimetres over millions of years as demonstrated for oxygen in high-pressure and ultra-high-pressure rocks (Philippot and Rumble 2000; Foland 1979). Radiogenic argon produced in potassium bearing minerals above their closure temperatures would accumulate in the grain boundary network and quickly reach levels where significant quantities partition into the minerals (e.g., Baxter et al. 2002; Foland 1979; Kelley and Wartho 2000). The two different occurrences of excess argon, in open and closed systems, are mirrored in the argon contents of quartz (fluid inclusions). Where quartz has been analyzed, excess argon concentrations signal excess argon in other minerals in fluid-rich environments (e.g., Vance et al. 1998; Kendrick et al. 2001a, b) though in fluid-poor environments, they exhibit lower excess argon contents than co-existing micas (Arnaud and Kelley 1995; Sherlock et al. 1999; Sherlock and Kelley 2002).

Although these two modes of occurrence are very different, both can be successfully modeled by considering argon as a trace element partitioning between fluid and solid using the measured argon solubility. K-feldspar is a good example for a simple model since some solubility data are available (Wartho et al. 1999; Wartho and Kelley unpubl. data) and it is one of the most common potassium bearing minerals used in K-Ar and Ar-Ar dating (cf. McDougall and Harrison 1999).

Excess argon in open systems. Argon solubility in saline waters has been measured precisely only at low temperatures (Smith and Kennedy 1983; Kipfer et al. 2002, this volume), but argon solubility at high temperatures can be estimated by extrapolating the salinity data in proportion with the high-temperature solubility data. Such extrapolation indicates that argon solubility in pure and saline grain boundary fluids up to 300°C (peak closure temperature for K-feldspar grains) lies in the range 25 to 100 ppm bar⁻¹ atm⁻¹. The large range reflects uncertainty in these values but they serve to constrain the model. The solubility of argon in K-feldspar is 0.66 ppb bar⁻¹ atm⁻¹ (data derived from Wartho et al. 1999) thus the D_{Ar} for the K-feldspar grain boundary fluid system lies in the range 6.6×10^{-6} to 2.6×10^{-5} . Figure 10 illustrates concentrations of excess argon in K-feldspar (expressed as the increase in age they would cause in an orthoclase K-feldspar) in equilibrium with variable concentrations of argon in the corresponding grain boundary fluid. The shaded area indicates concentrations of (atmospheric) argon found in near surface ground waters and some deeper waters (Smith and Kennedy 1983; Torgersen et al. 1989; Kipfer et al. 2002, this volume). More extreme concentrations of excess argon are found in hydrothermal fluids and in fluid inclusions which range up to 21 ppm (Burgess et al. 1992; Harrison et al. 1993; Harrison et al. 1994; Kelley et al. 1986; Turner and Wang 1992). If such concentrations of excess argon were introduced into grain boundary fluids in the model, they would increase the apparent ages of K-feldspar

samples by less than 0.6 Ma. Even if 100 ppm of excess argon was introduced into the model fluid, K-feldspar ages would rise by only 4 Ma. Therefore in the huge majority of cases, the level of excess argon in K-feldspar will be 1 to 2 orders of magnitude below detection limits (around 0.1 Ma in a 100-Ma K-feldspar). Even when excess argon is present in fluids at the highest levels measured in the upper crust, excess argon in K-feldspar would be a minor component in most analyzed samples. This observation corroborates the many measurements showing that excess argon is uncommon in K-feldspar, much of the excess argon which is detected in K-feldspar is confined to fluid inclusions (Burgess et al. 1992; Harrison et al. 1994).

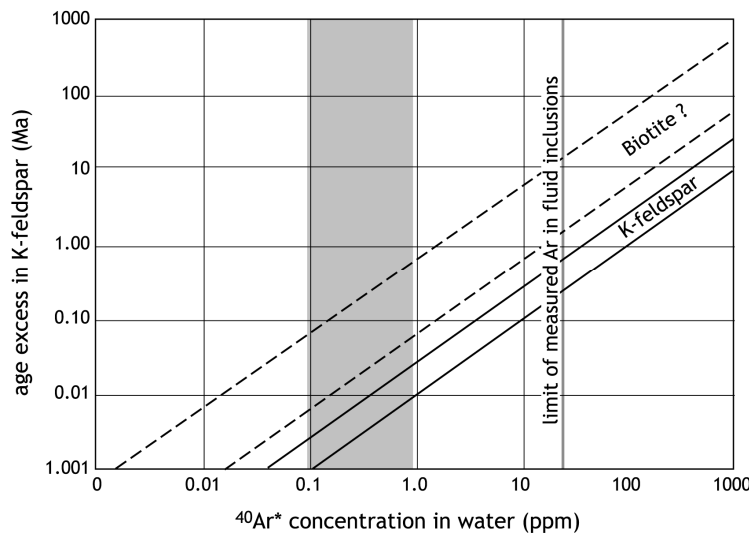


Figure 10. A plot of age excess vs ^{40}Ar concentration in the grain boundary fluid for an open system. Solid lines are those derived from the mineral/fluid partition coefficients (6.6×10^{-6} to 2.6×10^{-5}) for K-feldspar, dashed lines are those for another mineral with higher partition coefficients such as biotite. The shaded area indicates concentrations of (atmospheric) argon found in near surface ground waters and some deeper waters (Smith and Kennedy 1983; Torgersen et al. 1989; Kipfer et al. 2002, this volume). The vertical line indicates the current limit of excess argon concentration found in crustal fluids (Harrison et al. 1994).

The model confirms how robust the Ar-Ar system is when applied to K-feldspar, but minerals with higher mineral/fluid partition coefficients such as biotite will behave differently in a similar system. Note that biotite has been shown to yield ages over 100 Ma older than the expected age (e.g., Brewer 1969; Smith et al. 1994) and several studies describe excess ages in biotite but not in co-existing muscovite (e.g., Roddick et al. 1980). Roddick et al. (1980) argued that this reflected greater solubility of argon in biotite, an observation corroborated by crystal chemical (ionic porosity) arguments that argon solubility in biotite should be higher than muscovite (Dahl 1996). The dashed lines on Figure 10 illustrate the behavior of a mineral with a partition coefficient of 1×10^{-3} and similar radiogenic argon concentrations in grain boundary fluids to those seen in fluid inclusions. Such a mineral would commonly yield ages of the order of 1 Ma older than the true closure age but under extreme excess argon conditions, might yield ages more than 100 Ma older than the true closure age (compared with 4 Ma for K-feldspar in the same fluid). Where fluids are derived from basement rocks in fluid-rich regimes such as orogenic thrust belts, excess argon is unsurprisingly common (Brewer 1969; Kelley 1988; Smith et al. 1994; Reddy et al. 1996; Vance et al. 1998). The widespread influx of fluids in such regimes is illustrated by the occurrence of excess argon over broad areas (e.g., Brewer et al. 1969; Smith et al. 1994).

Excess argon in closed systems. Modeling excess argon in a closed system is less well constrained since there are no measured argon solubilities in hydrous fluids at high temperatures and even the presence of a fluid on the grain boundaries of such rocks may amount to an absorbed OH-layer or a CO₂-rich fluid. Further, any fluids which were present may have been isolated in pores or as grain edge tubules (Holness 1997) and are likely to have existed only transiently. However, the model illustrates how excess argon develops in a system without an infinite reservoir of hydrous fluid or melt. The same K-feldspar/fluid system used in the previous section can also be used to investigate the behavior of argon in fluid-poor systems. In a closed system, the controlling factors on the distribution of excess argon between K-feldspar and fluid are temperature, fluid salinity, the volume fraction of fluid (as a ratio of the total volume of the rock), and potassium content or K-feldspar content of the whole rock.

In fluid-rich systems such as porous sandstones in a basin environment, porosity might reach several percent, but in metamorphic rocks, porosity generally decreases with increasing grade to as low as 0.01% (10^{-4} vol fraction) in dry systems (Holness 1997). In order to model a closed system, zero radiogenic and excess argon concentrations are initially assumed in both fluid and minerals. In natural systems there may be pre-existing radiogenic argon in minerals or fluid inclusions, particularly when the rocks have a polymetamorphic history and the boundary between excess argon and inherited argon becomes blurred in these cases (e.g., Li et al. 1994). This model system uses the same range of K-feldspar/fluid partition coefficients (6.6×10^{-6} to 2.6×10^{-5}) to account for salinity variations and was run for rocks with 1 to 100% K-feldspar. Argon is assumed to be even more incompatible in any other mineral phases within the rock. As the model runs, excess argon builds up in K-feldspar as radiogenic argon is produced by ⁴⁰K decay. Unlike the open system, the fluid “reservoir” is finite and after a while radiogenic argon increases to the level where partition back into the K-feldspar becomes detectable. The fractional age excess has been calculated for fluid filled porosity of 1%, 0.1% and 0.01%. Figure 11 shows that samples with greater than 0.1% porosity do not generate significantly old ages in K-feldspar. If the porosity is 0.1%, excess argon in the same K-feldspar would yield ages as much as 1.5 Ma too old in a 100 Ma rock with 100% K-feldspar rock, but only 0.03 to 0.8 Ma in the same age rock with 5 to 30% K-feldspar (common to crustal rocks such as granite). In all probability this would still be below detection levels. Only in the most fluid-poor systems with 0.01% porosity, does the system start to exhibit detectable excess argon with up to 8 Ma excess argon in a rock with 30% 100 Ma old K-feldspar, and even in this case only the most K-feldspar-rich rocks containing very saline fluids will produce detectable excess argon. Furthermore, in this model it was assumed that the other minerals in the rock exhibited lower argon solubility but if another mineral such as biotite (with higher partition coefficient) is present, excess argon concentrations in K-feldspar quickly drop below detection levels even in the most fluid-poor terrains (e.g., Foland 1979). K-feldspar ages measured in eclogite terrains which exhibit closed system excess argon in phengite (Arnaud and Kelley 1995), sometimes reveal high-temperature excess argon, but this may also result from plagioclase or inclusions outgassing during the cycle-heating experiment (Arnaud and Kelley 1995; Boven et al. 2001).

It is not clear how rigorously this model can be applied to the most fluid-poor rocks since the grain boundary fluid phase in dry systems such as eclogites and granulites may be as little as a layer of OH- molecules at the grain boundaries. However, the model serves to illustrate how a closed system can explain phenomena observed in high-pressure and ultra-high-pressure terrains, particularly the occurrence of excess argon in phengite when it is the predominant potassium-bearing mineral in the rock. In several UHP terrains, it has been noted that excess argon is more prevalent in rocks with

protracted histories or old protoliths (Li et al. 1994; Arnaud and Kelley 1995; Inger et al. 1996; Giorgis et al. 2000). Although much of this 'inherited argon' will partition into the limited fluid phase, excess argon is more likely in rocks with older protoliths. Another prediction of a closed system model is that potassium-rich rocks will contain greater concentrations of excess argon than potassium-poor rocks, even when only one potassium bearing mineral phase is present (e.g., Sherlock and Kelley 2002). Ironically, in fluid-poor high-pressure rocks it would be more appropriate to measure ages from low-K metabasalts or meta-sandstones rather than mica-rich schists or K-feldspar-rich rocks.

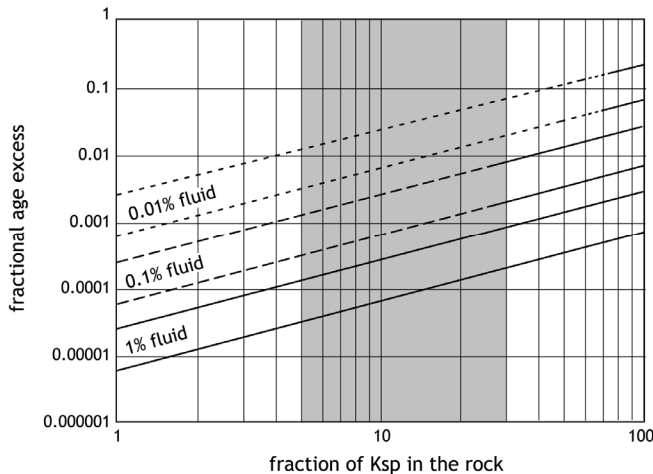


Figure 11. A plot of age excess vs. ^{40}Ar concentration in the grain boundary fluid for a closed system. Solid lines are those derived from the mineral/fluid partition coefficients (6.6×10^{-6} to 2.6×10^{-5}) for K-feldspar in a rock with 1% fluid. Dashed lines are those for the same rock with 0.1% fluid and the dashed/dotted lines are those for a rock with 0.01% fluid. The shaded area represents the range of rock compositions from which K-feldspar is commonly analyzed (5 to 50%).

In summary, the presence of excess argon in most crustal fluids means that assumption No. 3 of the K-Ar and Ar-Ar may never be strictly valid, but in the majority of cases, the concentration of excess argon in minerals is swamped by the *in situ* radiogenic component and is not a factor in determining an accurate age.

Excess argon in fluid and melt inclusions. There is considerable overlap between the studies of excess argon in minerals and crustal noble gas studies (Ballentine and Burnard 2002; Ballentine and Marty 2002, both in this volume) in studies of fluid and melt inclusions. The recent publications of Kendrick et al. (2001a, b) demonstrate just how close the two sets of studies have become. Fluid inclusions and melt inclusions are commonly important sources of excess argon in minerals analyzed for K-Ar and Ar-Ar dating, particularly in low potassium minerals such as amphibole and plagioclase. The simple reason for the importance of fluid and melt inclusions is illustrated by Figure 11. Melt inclusions incorporated from a magma containing excess argon will contain ~100 times more argon than minerals crystallising from the same melt, and fluid inclusions in equilibrium may contain as much as 10,000 times the excess argon concentration (by weight) of the mineral structure. Inclusions provide some of the most intractable analytical problems in K-Ar and Ar-Ar dating although they can also occasionally be used to advantage in preserving mineral ages (e.g., Kelley et al. 1997; van der Bogaard and Schirnick 1995). Cumbest et al. (1994) showed how the interaction of metamorphic fluids could result in different generations of excess argon in fluid inclusions and Harrison et al. (1994) showed that fluid inclusions were present in many K-feldspar samples but repeated cycles of step heating could reduce and correct for their effects.

Melt inclusions are common in mineral separates used to date volcanic and hyperbyssal rocks, but have received little attention. However, the effects of melt inclusions from a historic flow on Mount Erebus were studied by Esser et al. (1997) showing that their presence resulted in saddle-shaped age spectra during stepped ^{39}Ar release (Fig. 7a).

APPLICATIONS

The applications cited here focus upon the Ar-Ar dating technique, simply because most recent developments have utilized the Ar-Ar dating technique. The aim of this section is to highlight applications which illustrate the breadth of problems which have been addressed using Ar-Ar dating.

Thermochronology

The diffusion of radiogenic noble gas daughter products provides several routes for determining not only the chronology of events but also thermal histories (e.g., Swindle 2002; Farley 2002, both in this volume). One of the most common applications of Ar-Ar geochronology has been dating mineral grains or mineral separates in order to study cooling and uplift in metamorphic terrains. Often in the past, these ages were combined with U-Pb and Rb-Sr ages in order to produce cooling histories using mineral closure temperatures based upon laboratory diffusion determinations (e.g., Foland 1974; Grove and Harrison 1996) or field estimates (e.g., Kirschner et al. 1996; Purdy and Jäger 1976). However, after the success of unravelling the thermal histories of lunar samples (see Turner 1977 for a full review), and the many studies on thermal histories of meteorites (Turner 1969, 1970a), step heating was applied to terrestrial samples. As Turner (op cit) showed, the diffusion parameters of a mineral can be recovered from the release of ^{39}Ar during the step heating procedure, and combined with age information to deduce a thermal history. The results of applying this technique to terrestrial samples have been mixed. While step heating can discriminate against contamination by mixed phases, thermal histories are rarely extracted from hydrous minerals since the minerals become unstable long before they melt, releasing argon not only from outer layers but along cleavages parted by explosive loss of water in biotite (Gaber et al. 1988) or via breakdown reactions in the case of amphibole (Lee 1993; Lee et al. 1991; Wartho 1995; Wartho et al. 1991) and biotite (Lo et al. 2000). However this aspect has recently been exploited (Belluso et al. 2000), using the preferential breakdown of different amphibole compositions in an attempt to date the formation of separate generations.

Feldspars do not break down during short term *in vacuo* heating experiments prior to melting since they are anhydrous, and thus do not suffer the same effects as hydrous minerals. However, the complex sub-solidus reactions and exsolution in plagioclase feldspar means that Ar-Ar step heating generally reflects mixed phases, and interpretation may be difficult (e.g., Boven et al. 2001). Stepwise heating of K-feldspar on the other hand, provides an opportunity to explore thermal histories without the need to resort to other isotope systems or even other minerals. The microstructure of K-feldspar is relatively simple in volcanic rocks, but in plutonic and basement rocks, progressive episodes of reaction during cooling result in complex microtexture of intergrowths and exsolution (Parsons et al. 1999). Plutonic and basement feldspars are thus composed of many variably sized and shaped diffusion domains within single grains of K-feldspar, some as small as a micron. The bulk closure temperature of large K-feldspar grains would be around 300°C if they acted as whole grains (cf. Foland 1974) but in fact the 'effective' closure temperature is closer to 150-200°C, and this is the reason why they were regarded as "leaky" by early workers. Several workers suggested that argon loss from K-feldspars might be the result of variable sub-grain sizes, but it was not until Lovera et al. (1989, 1991) that this effect was quantified using cycled heating steps designed to preferentially outgas different diffusion domain sizes, rather than the standard monotonic temperature increase normally used in step heating. Lovera et al. (1989, 1991) also formulated a mathematical model using the deviation of the ^{39}Ar release from a simple Arrhenius relationship, to monitor argon diffusion in domains of differing sizes. The individual step Ar-Ar ages were then combined with derived diffusion information to

produce a continuous thermal history over a range of as much as 200°C. This was a considerable advance over a single meaningless closure temperature. In their initial work, Lovera et al. used an age spectrum to monitor the cooling of the Chain of Ponds Pluton in northwestern Maine (Fig. 12), showing that the age spectrum could not be modeled using a single diffusion domain but that a reasonably good fit could be achieved using three domains of different sizes (i.e., diffusion radii) and specific volume fractions.

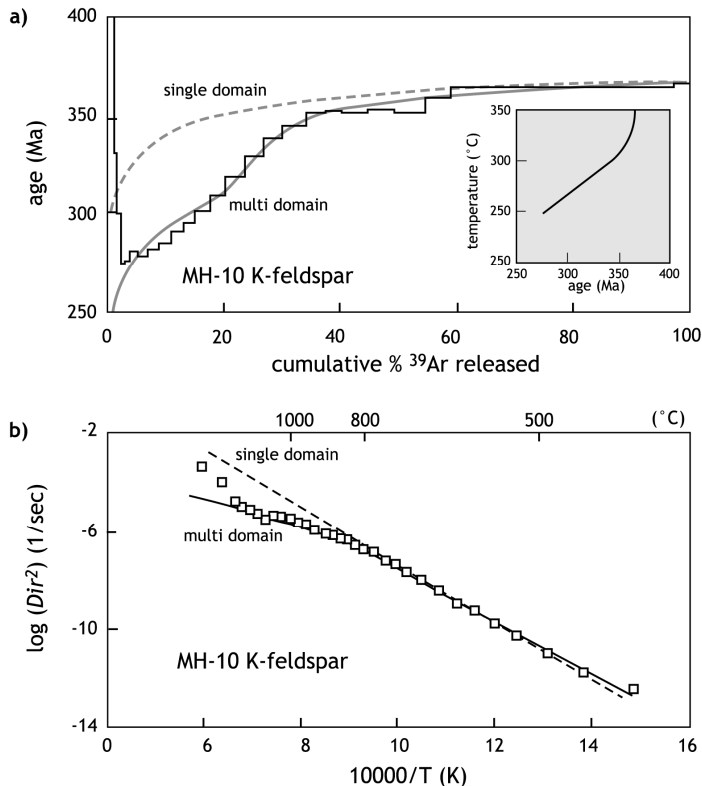


Figure 12. Cycle heating results for a K-feldspar sample from the Chain of Ponds pluton (Lovera et al. 1989), showing the fit of modeled argon release for a single diffusion domain lines and the improved fit which can be obtained by using three diffusion domains. The lower figure shows the departure of argon diffusion from a simple Arrhenius relationship.

A great deal of discussion of multi-domain modeling (MDD) has ensued mainly surrounding the diffusion mechanisms (Arnaud and Kelley 1997; Harrison et al. 1991; Lovera et al. 1989, 1991, 1993, 1997; McDougall and Harrison 1999; Villa 1994; Wartho et al. 1999) and the physical reality of the diffusion domain sizes used in the model (Arnaud and Eide 2000; Burgess et al. 1992; FitzGerald and Harrison 1993; Lovera et al. 1989, 1991, 1993; Parsons et al. 1999; Reddy et al. 2001a). The model has also evolved considerably since its inception with the use of an increasing number of discrete diffusion domain sizes (e.g., Mock et al. 1999a,b), evocation of multiple activation energies (Harrison et al. 1991) which was later discontinued, a realization that fluid inclusions played an important role in apparent excess argon seen at low temperatures (Turner and Wang 1992; Burgess et al. 1992; Harrison et al. 1993, 1994), and more recently focus on the low-temperature release to determine an activation energy used throughout (Lovera et al. 1997) since higher temperatures may be affected by pre-melting and other artifacts. Monte Carlo inversion techniques have also been used to define domain sizes and thermal histories (Warnock and Zeitler 1998; Lovera et al. 1997) and there has been discussion of the effects of recoil in very small domains upon the release patterns and their interpretation (Onstott et al. 1995; Villa 1997).

If the MDD technique had produced no useful information, the controversy and constantly evolving modeling techniques would have dissuaded workers from applying it to geological problems. However, as McDougall and Harrison (1999) document, the cycle-heating MDD model technique has resulted in reasonable thermal histories in a

wide range of geological situations. Moreover, McDougall and Harrison (1999) set out a full set of testable assumptions and techniques for accepting or rejecting data. In summary, the cycle-heating technique must be undertaken with great care and awareness of the potential advantages and pitfalls.

The cycle-heating MDD modeling technique offers the chance to extract thermal information from bulk K-feldspar separates, but what of hydrous minerals such as micas and amphiboles? In fact, laser spot dating has succeeded in imaging age profiles in micas and amphiboles where step heating failed to produce thermal histories (e.g., Kelley and Turner 1991; Lee et al. 1991; Phillips and Onstott 1988; Scaillet et al. 1990), demonstrating that hydrous minerals do retain thermal information (Fig. 13). Laser age profiles have been used to address a range of geological problems including; heat loss from igneous intrusions (Kelley and Turner 1991; Wartho et al. 2001); slow cooling in metamorphic terrains (Hames and Cheney 1997); ingress of excess argon (Scaillet et al. 1990; Scaillet 1996; Pickles et al. 1997; Ruffet et al. 1991, 1997; Sherlock et al. 1999; Giorgis et al. 2000) and the relationship between deformation and Ar-Ar ages (Reddy et al. 1996, 1997, 2001). UV lasers have been used to measure experimentally produced argon diffusion profiles at a spatial resolution of as little as 1 micron (Arnaud and Kelley 1997; Wartho et al. 1999) and measure argon crystal/melt partition coefficients (Brooker et al. 1998; Chamorro et al. 2002). The advantage of such studies is that, unlike step heating, they provide images of the argon distribution within grains, showing the effect of sub-grain boundaries and compositional effects. The disadvantage is that spatial resolution and the range of suitable samples are limited by the gas required for precise isotope measurement—in other words, older samples and larger grains.

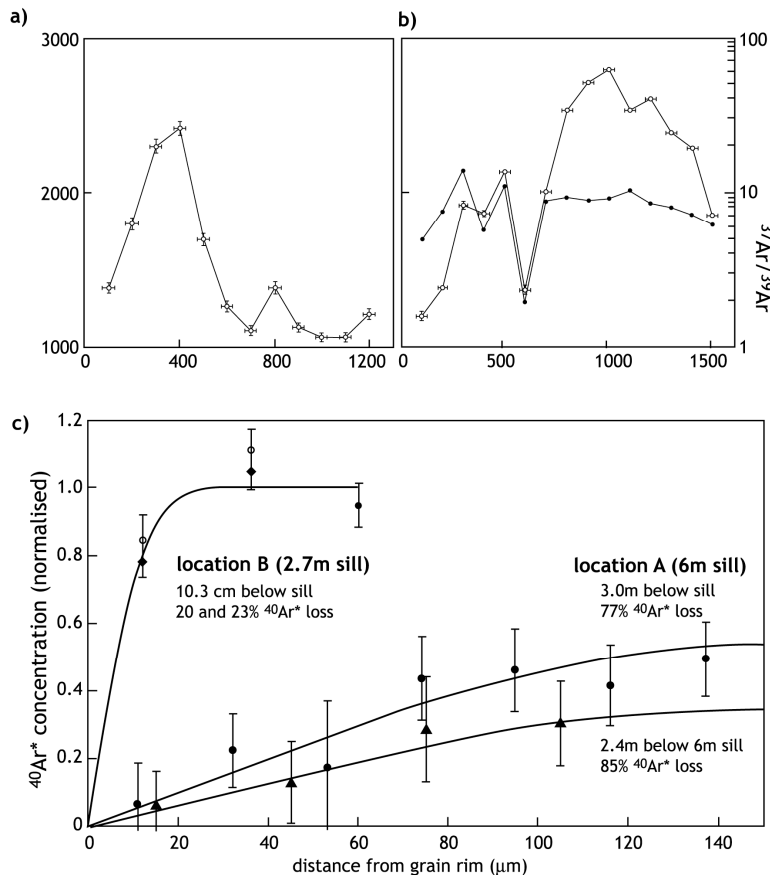


Figure 13. Ar-Ar age profiles from micas and amphiboles showing Ar loss or gain by diffusion which has been modeled to recover the thermal history of the sample. (a),(b) show two-amphibole grains from a rock close to the Duluth Gabbro. The age profiles show diffusion domains defined by the presence of biotites in the outer zone of the grains (Note the Ca/K monitored by $^{37}\text{Ar}/^{39}\text{Ar}$ on the right). Both domains yielded the same time-integrated diffusion parameters (Kelley and Turner 1991). (a) A small domain within the grain has suffered 78% argon loss. (b) A larger domain showing only 43% Ar loss. (c) Ar-loss profiles from biotite grains close to a sill on the Isle of Mull, Scotland, outgassed to varying

extents dependent upon distance from two sills, one sill was 2.7 m wide, the other was 6 m wide. The variable outgassing was used to produce a magma flow history for the sill (Wartho et al. 2001).

Dating young volcanic eruptions

K-Ar and Ar-Ar have long been used to date young (Pre-historic) volcanic eruptions (cf. Curtis in Schaeffer and Zähringer 1966) but in recent years, the advent of low blank furnaces and laser extraction techniques, particularly the CO₂ laser, have pushed the boundaries. It remains unclear whether laser extraction or furnace extraction is the superior technique for very young volcanic samples. Lasers offer slightly lower blanks, though the quantities of sample can be too large for focussed laser extraction (>0.5 g in some cases), but furnaces offer better temperature control. In a study of zero age samples Esser et al. (1997) showed that anorthoclase samples suffered small amount of excess argon which were better discriminated using the furnace extraction technique. There are particular analytical challenges offered by dating young volcanic samples, including precise calibration of the mass spectrometer since many samples contain only small amounts of radiogenic argon. Contamination and control of the sample quality is also particularly difficult since sample sizes are often 0.1-1 g. Finally, melting large quantities of sample also produces large quantities of H₂O, CO₂ and other gases released from minerals, and requires larger getters to clean the gas prior to mass spectrometric measurement of isotope ratios.

The ages of the youngest volcanic rocks dated by the Ar-Ar technique have now reached the historic realm. For example, Renne et al. (1997) have measured the age of the Vesuvius eruption observed and recorded by Pliny in 79 AD. Other work has focussed upon dating human evolution (Deino et al. 1998; Ludwig and Renne 2000; Renne et al. 1997), the relationship between volcanic eruptions and recent climate change (Ton-That et al. 2001), glacial advances (Singer et al. 2000; Wilch et al. 1999), and precise calibration of young magnetic reversals (e.g., Singer and Pringle 1996).

High-precision ages on altered basalts

One of the reasons why precision of the standards and problems of the decay factors used for Ar-Ar dating came to light was the push to achieve high precision ages for huge flood basalt provinces, which have been linked by some workers to climate change and global mass extinctions. A great deal of effort has gone into analytical techniques and protocols in order to obtain high precision ages for flood basalts (e.g., Foland et al. 1993; Hofmann et al. 2000; Min et al. 2000; Renne 1995; Renne and Basu 1991; Renne et al. 1992, 1995, 1996a,b; Storey et al. 1995; Duncan et al. 1997) this work also contributed strongly to the problems concerning accuracy and precision, decay constants and international standards as a result. Precision (excluding decay and standard errors), even on samples with low potassium are commonly less than 0.5%, sometimes as low as 0.25%. In addition, analytical techniques involving acid clean-up have been developed to analyse extremely difficult samples from the sea floor (Pringle et al. 1991).

Dating low-temperature processes

Both the K-Ar and Ar-Ar techniques have been used to date low-temperature phases such as clay minerals and in particular the mineral illite. The problem for Ar-Ar dating of such phases is that recoil of ³⁹Ar during neutron irradiation can compromise the measured age. In fine grained phases such as clays, this can cause up to 30% ³⁹Ar loss by recoil and resulting ⁴⁰Ar*/³⁹Ar ratios, calculated without the recoiled ³⁹Ar are 30% too high. This problem has been overcome to some extent by encapsulating clay samples in evacuated silica vials, breaking the vials after irradiation, and measuring the amount of recoiled ³⁹Ar (e.g., Foland et al. 1983; Smith et al. 1993). More recently, Onstott et al. (1997) showed that the process could be miniaturized, using micro-ampoules and opening them with a UV laser. The technique has been utilized (Dong et al. 1995, 1997a,b) to investigate variations in argon retention properties of clays. Other low-temperature K-bearing

minerals such as cryptomelane and alunite have been used to date surface processes (Vasconcelos 1999), including the formation of ore gangue (Itaya et al. 1996; Vasconcelos 1999) and cave deposits (Polyak et al. 1998).

Ar-Ar dating of authigenic K-feldspar overgrowths has also been investigated using dissolution (Hearn et al. 1987), stepped heating (Mahon et al. 1998) and laser extraction (e.g., Girard and Onstott 1991) with varying success. Recent work using a UV laser extraction technique provides further evidence that such overgrowths can provide meaningful ages (Hagen et al. 2001).

Another growing field of work has been dating detrital minerals in sediments as a provenance tool, but also in order to study the sedimentary systems supplying basins and uplift or thermal history of the source. Clauer (1981) and Adams and Kelley (1998) have shown that while biotite is often quickly altered in the sedimentary environment, white micas survive and retain ages even in second cycle sediments (those which were originally deposited and then re-excavated during later basin inversions; e.g., Sherlock 2001). K-feldspar also retains pre-erosion cooling ages (e.g., Copeland et al. 1990) but the lower closure temperatures mean that it has more commonly been used for thermal analysis of sedimentary basins (e.g., Harrison and Be 1983).

Unique samples

The Ar-Ar dating technique depends only upon two isotopes of argon, and thus it is possible to analyse individual particles such as lunar soil grains (Burgess and Turner 1998), terrestrial sand grains (Kelley and Bluck 1989), and glass spherules (Culler et al. 2000). Ar-Ar dating has also successfully been used to date small amounts of heterogeneous samples, such as pseudotachylytes in fault zones (Kelley et al. 1994; Magloughlin et al. 2001; Muller et al. 2001), and even terrestrial meteorite impacts (Spray et al. 1995). Finally, in its earliest days the Ar-Ar dating was called upon to extract a great deal of temporal and thermal information from unique and precious moon rocks (Turner 1977; Swindle 2002, this volume), and this is still the case as demonstrated by the recent dating of the unique ALH84001 meteorite sample from Mars (Turner et al. 1997).

ACKNOWLEDGMENTS

The author was greatly assisted in writing this chapter by discussion with Sarah Sherlock. John Taylor kindly drew the figures. Paul Renne, Nicolas Arnaud, Matt Heizler and Mike Cosca provided detailed and insightful reviews which greatly improved the text. Rainer Wieler spotted the many mistakes and typos.

REFERENCES

- Adams CJ, Kelley SP (1998) Provenance of Permian-Triassic and Ordovician metagreywake terranes in New Zealand: Evidence from $^{40}\text{Ar}/^{39}\text{Ar}$ dating of detrital micas. *Geol Soc Am Bull* 110:422-332
- Aldrich LT, Nier AO (1948) Argon 40 in potassium minerals. *Phys Rev* 74:876-877
- Alexander ECJ, Mickelson GM, Lanphere MA (1978) MMhb-1: A new ^{40}Ar - ^{39}Ar dating standard. U S Geol Surv Open-file Rept 70-701:6-8
- Allen AR, Stubbs D (1982) An $^{40}\text{Ar}/^{39}\text{Ar}$ study of a polymetamorphic complex in the Arunta Block, central Australia. *Contrib Mineral Petrol* 79:319-332
- Arnaud NO, Kelley SP (1995) Evidence for widespread excess argon during high-pressure metamorphism in the Dora Maira (Western Alps, Italy), using an ultra-violet laser ablation microprobe $^{40}\text{Ar}/^{39}\text{Ar}$ technique. *Contrib Mineral Petrol* 121:1-11
- Arnaud NO, Kelley SP (1997) Argon behavior in gem-quality orthoclase from Madagascar: Experiments and some consequences for Ar-40/Ar-39 geochronology. *Geochim Cosmochim Acta* 61:3227-3255
- Arnaud NO, Eide EA (2000) Brecciation-related argon redistribution in alkali feldspars: An in naturo crushing study. *Geochim Cosmochim Acta* 64:3201-3215

- Audi G, Bersillon O, Blachot J, Wapstra AH (1997) The NUBASE evaluation of nuclear and decay properties. *Nucl Phys A* 624:1-124
- Baksi AK (1994) Geochronological Studies On Whole-Rock Basalts, Deccan Traps, India—Evaluation of the Timing of Volcanism Relative to the K-T Boundary. *Earth Planet Sci Lett* 121:43-56
- Ballentine CJ, Burnard P (2002) Production and release of noble gases in the continental crust. *Rev Mineral Geochem* 47:481-538
- Ballentine CJ, Marty B (2002) Tracing fluid origin, transport and interaction in the crust. *Rev Mineral Geochem* 47:539-614
- Baxter EF, DePaulo DJ, Renne PR (2002) Spatially correlated Anomalous $^{40}\text{Ar}/^{39}\text{Ar}$ “Age” Variations in Biotites about a lithologic contact near Simplon Pass, Switzerland: A mechanistic explanation for “excess Ar”. *Geochim Cosmochim Acta* 66:1067-1083
- Beckinsale RD, Gale NH (1969) A reappraisal of the decay constants and branching ratio of ^{40}K . *Earth Planet Sci Lett* 6:289-294
- Begemann F, Ludwig KR, Lugmair GW, Min K, Nyquist LE, Patchett PJ, Renne PR, Shih CY, Villa IM, Walker RJ (2001) Call for an improved set of decay constants for geochronological use. *Geochim Cosmochim Acta* 65:111-121
- Belluso E, Ruffini R, Schaller M, Villa IM (2000) Electron-microscope and Ar isotope characterization of chemically heterogeneous amphiboles from the Palala Shear Zone, Limpopo Belt, South Africa. *Eur J Mineral* 12:45-62
- Boven A, Pasteels P, Kelley SP, Punzalan L, Bingen B, Demaiffe D (2001) $^{40}\text{Ar}/^{39}\text{Ar}$ study of plagioclases from the Rogaland anorthosite complex (SW Norway); an attempt to understand argon ages in plutonic plagioclase. *Chem Geol* 176:105-135
- Brewer MS (1969) Excess Radiogenic Argon in Metamorphic Micas from the Eastern Alps, Austria. *Earth Planet Sci Lett* 6:321-331
- Brooker RA, Wartho J-A, Carroll MR, Kelley SP, Draper DS (1998) Preliminary UVLAMP determinations of argon partition coefficients for olivine and clinopyroxene grown from silicate melts. *Chem Geol* 147:185-200
- Burgess R, Turner G (1998) Laser argon-40-argon-39 age determinations of Luna 24 mare basalts. *Meteorit Planet Sci* 33:921-935
- Burgess R, Kelley SP, Parsons I, Walker FDL, Wordon RH (1992) ^{40}Ar - ^{39}Ar analysis of perthite microtextures and fluid inclusions in alkali feldspars from the Klokken syenite, South Greenland. *Earth Planet Sci Lett* 109:147-167
- Carroll MR, Draper DS (1994) Noble gases as trace elements in magmatic processes. *Chem Geol* 117:37-56
- Cebula GT, Kunk MJ, Mehnert HH, Naser CW, Obradovich JD, Sutter JF (1986) The Fish Canyon Tuff, a potential standard for the ^{40}Ar - ^{39}Ar and fission track dating methods. *Terra Cognita (abstr)* 6:139-140
- Chamorro EM, Brooker RA, Wartho J-A, Wood BJ, Kelley SP, Blundy JD (2002) Ar and K partitioning between clinopyroxene and silicate melt to 8 GPa. *Geochim Cosmochim Acta* 66:507-519
- Clauer N (1981) Strontium and argon isotopes in naturally weathered biotites, muscovites and K-feldspars. *Chem Geol* 31:325-334
- Copeland P, Harrison TM, Heizler MT (1990) $^{40}\text{Ar}/^{39}\text{Ar}$ single-crystal dating of detrital muscovite and K-feldspar from Leg 116, Southern Bengal Fan: Implications for the uplift and erosion of the Himalayas. *Proc Ocean Drill Progr* 116:93-114
- Copeland P, Harrison TM, Kidd WSF, Ronghua X, Yuquan Z (1987) Rapid early Miocene acceleration of uplift in the Gandese Belt, Xizang (southern Tibet), and its bearing on accommodation mechanisms of the India-Asia collision. *Earth Planet Sci Lett* 86:240-252
- Culler TS, Becker TA, Muller RA, Renne PR (2000) Lunar impact history from Ar-40/Ar-39 dating of glass spherules. *Science* 287:1785-1788
- Cumbest RJ, Johnson EL, Onstott TC (1994) Argon composition of metamorphic fluids: Implications for $^{40}\text{Ar}/^{39}\text{Ar}$ geochronology. *Geol Soc Am Bull* 106:942-951
- Dahl PS (1996) The crystal-chemical basis for Ar retention in micas: Inferences from interlayer partitioning and implications for geochronology. *Contrib Mineral Petrol* 123:22-39
- Dalrymple GB, Lanphere MA. (1969) Potassium-Argon Dating, Principle Techniques and Applications to Geochronology. Freeman and Co., San Francisco, 258 p
- Dalrymple DG, Moore JG (1968) Argon 40: Excess in submarine pillow basalts from Kilauea Volcano, Hawaii. *Science* 161:1132-1135
- Dalrymple GB, Grommé CS, White RW (1975) Potassium-argon age and paleomagnetism of diabase dykes in Liberia: Initiation of central Atlantic rifting. *Bull Geol Soc Am* 86:399-411
- Damon PE, Kulp JL (1958) Excess helium and argon in beryl and other minerals. *Am Mineral* 43:433-459
- Deino AL, Renne PR, Swisher CC (1998) Ar-40/Ar-39 dating in paleoanthropology and archeology. *Evol Anthropol* 6:63-75

- Dickin AP. (1995) Radiogenic Isotope Geology. Cambridge University Press, Cambridge, UK, 490 p
- Dodson MH (1973) Closure temperature in cooling geochronological and petrological systems. *Contrib Mineral Petrol* 40:259-274
- Dodson MH (1986) Closure profiles in cooling systems. *Mater Sci Forum* 7:145-154
- Dong HL, Hall CM, Peacor DR, Halliday AN (1995) Mechanisms of Argon Retention in Clays Revealed By Laser Ar-40- Ar-39 Dating. *Science* 267:355-359
- Dong HL, Hall CM, Halliday AN, Peacor DR (1997a) Laser Ar-40-Ar-39 dating of microgram-size illite samples and implications for thin section dating. *Geochim Cosmochim Acta* 61:3803-3808
- Dong HL, Hall CM, Halliday AN, Peacor DR, Merriman RJ, Roberts B (1997b) Ar-40/Ar-39 illite dating of Late Caledonian (Acadian) metamorphism and cooling of K-bentonites and slates from the Welsh Basin, UK. *Earth Planet Sci Lett* 150:337-351
- Duncan RA, Hooper PR, Rehacek J, Marsh JS, Duncan AR (1997) The timing and duration of the Karoo igneous event, southern Gondwana. *J Geophys Res-Solid Earth* 102:18127-18138
- Endt PM, Van der Leun C (1973) Energy levels of A = 21-44 nuclei (V). *Nucl Phys A* 214:1-625
- Esser RP, McIntosh WC, Heizler MT, Kyle PR (1997) Excess argon in melt inclusions in zero-age anorthoclase feldspar from Mt Erebus, Antarctica, as revealed by the $^{40}\text{Ar}/^{39}\text{Ar}$ method. *Geochim Cosmochim Acta* 61:3789-3801
- Farley KA (2002) (U-Th)/He dating: techniques, calibrations, and applications. *Rev Mineral Geochem* 47:819-845
- Farrar E, Macintyre RM, York D, Kenyon WJ (1964) A simple mass spectrometer for the analysis of argon at ultra-high vacuum. *Nature*, p 531-533
- Feraud G, Courtillot V (1994) Did Deccan volcanism pre-date the Cretaceous-Tertiary transition?— Comment. *Earth Planet Sci Lett* 122:259-262
- Fitz Gerald JD, Harrison TM (1993) Argon diffusion domains in K-feldspar: I. Microstructures in MH-10. *Contrib Mineral Petrol* 113:367-380
- Foland KA (1974) Ar^{40} diffusion in homogenous orthoclase and an interpretation of argon diffusion in K-feldspars. *Geochim Cosmochim Acta* 38:151-166
- Foland KA (1979) Limited mobility of argon in a Metamorphic Terrain. *Geochim Cosmochim Acta* 43:793-801
- Foland KA (1983) $^{40}\text{Ar}/^{39}\text{Ar}$ incremental heating plateaus for biotites with excess argon. *Chem Geol (Isotop Geosci Sect)* 1:3-21
- Foland KA, Linder JS, Laskowski TE, Grant NK (1983) $^{40}\text{Ar}/^{39}\text{Ar}$ dating of glauconites; measured ^{39}Ar recoil loss from well-crystallized specimens. *Chem Geol (Isotop Geosci Sect)* 2:241-264
- Foland KA, Fleming TH, Heimann A, Elliot DH (1993) Potassium-argon dating of fine-grained basalts with massive argon loss: Applications of the $^{40}\text{Ar}/^{39}\text{Ar}$ technique to plagioclase and glass from the Kirkpatrick Basalt, Antarctica. *Chem Geol (Isotop Geosci Sect)* 107:173-190
- Foster DA, Harrison TM, Copeland P, Heizler MT (1990) Effects of excess argon within large diffusion domains on K-feldspar age spectra. *Geochim Cosmochim Acta* 54:1699-1708
- Gaber LJ, Foland KA, Corbató CE (1988) On the significance of argon release from biotite and amphibole during $^{40}\text{Ar}/^{39}\text{Ar}$ vacuum heating. *Geochim Cosmochim Acta* 52:2457-2465
- Garner EL, T.J. M, J.W. G, Paulsen PJ, Barnes IL (1975) Absolute isotopic abundance ratios and the atomic weight of a reference samples of potassium. *J Res Natl Bur Stand* 79A:713-725
- Giorgis D, Cosca MA, Li S (2000) Distribution and significance of extraneous argon in UHP eclogite (Sulu terrane, China): Insights from *in situ* $^{40}\text{Ar}/^{39}\text{Ar}$ UV-laser ablation analysis. *Earth Planet Sci Lett* 181:605-615
- Girard J-P, Onstott TC (1991) Application of $^{40}\text{Ar}/^{39}\text{Ar}$ laser-probe and step-heating techniques to the dating of diagenetic K-feldspar overgrowths. *Geochim Cosmochim Acta* 55:3777-3793
- Graham CM (2002) Noble gas isotope geochemistry of mid-ocean ridge and ocean island basalts: characterization of mantle source reservoirs. *Rev Mineral Geochem* 47:247-318
- Grove M, Harrison TM (1996) $^{40}\text{Ar}^*$ diffusion in Fe-rich biotite. *Am Mineral* 81:940-951
- Hagen E, Kelley SP, Dypvik H, Nilsen O, Kjolhamar B (2001) Direct dating of authigenic K-feldspar overgrowths from the Kilombero Rift of Tanzania. *J Geol Soc* 158:801-807
- Hames WE, Cheney JT (1997) On the loss of Ar-40* from muscovite during polymetamorphism. *Geochim Cosmochim Acta* 61:3863-3872
- Harrison TM, McDougall I (1980) Investigations of an intrusive contact, northwest Nelson, New Zealand: II. Diffusion of radiogenic and excess ^{40}Ar in hornblende revealed by $^{40}\text{Ar}/^{39}\text{Ar}$ age spectrum analysis. *Geochim Cosmochim Acta* 44:2005-2020
- Harrison TM, McDougall I (1981) Excess ^{40}Ar in metamorphic rocks from Broken Hill, New South Wales: Implications for $^{40}\text{Ar}/^{39}\text{Ar}$ age spectra and the thermal history of the region. *Earth Planet Sci Lett* 55:123-149

- Harrison TM, Be K (1983) Ar-40/Ar-39 age spectrum analysis of detrital microclines from the Southern San-Joaquin Basin, California—An approach to determining the thermal evolution of sedimentary basins. *Earth Planet Sci Lett* 64:244-256
- Harrison TM, Lovera OM, Heizler MT (1991) $^{40}\text{Ar}/^{39}\text{Ar}$ results for alkali feldspars containing diffusion domains with differing activation energies. *Geochim Cosmochim Acta* 55:1435-1448
- Harrison TM, Heizler MT, Lovera OM (1993) *In vacuo* crushing experiments and K-feldspar thermochronology. *Earth Planet Sci Lett* 117:169-180
- Harrison TM, Heizler MT, Lovera OM, Chen W, Grove M (1994) A chlorine disinfectant for excess argon released from K-feldspar during step heating. *Earth Planet Sci Lett* 123:95-104
- Hearn PP, Sutter JF, Belkin HE (1987) Evidence for Late-Paleozoic brine migration in Cambrian carbonate rocks of the central and southern Appalachians—Implications for Mississippi Valley-type sulfide mineralization. *Geochim Cosmochim Acta* 51:1323-1334
- Heizler MT, Harrison TM (1988) Multiple trapped argon isotope components revealed by $^{40}\text{Ar}/^{39}\text{Ar}$ isochron analysis. *Geochim Cosmochim Acta* 52:1295-1303
- Hodges KV, Hames WE, Bowring SA (1994) $^{40}\text{Ar}/^{39}\text{Ar}$ age gradients in micas from a high-temperature-low-pressure metamorphic terrain: Evidence for very slow cooling and implications for the interpretation of age spectra. *Geology* 22:55-58
- Hofmann C, Feraud G, Courtillot V (2000) Ar-40/Ar-39 dating of mineral separates and whole rocks from the Western Ghats lava pile: further constraints on duration and age of the Deccan traps. *Earth Planet Sci Lett* 180:13-27
- Holness MB (1997) The permeability of non-deforming rock. In Holness MB (ed) *Deformation-Enhanced Fluid Transport in the Earth's Crust and Mantle*. Chapman and Hall, London, p 9-39
- Humayun M, Clayton RN (1995a) Potassium isotope geochemistry: Genetic implications of volatile element depletion. 59:2131-2148
- Humayun M, Clayton RN (1995b) Precise determinations of the isotopic composition of potassium: Application to terrestrial rocks and lunar soils. *Geochim Cosmochim Acta* 59:2115-2130
- Inger S, Ramsbottom W, Cliff RA, Rex DC (1996) Metamorphic evolution of the Sesia-Lanzo Zone, Western Alps: Time constraints from multi-system geochronology. *Contrib Mineral Petrol* 126:152-168
- Itaya T, Arribas A, Okada T (1996) Argon release systematics of hypogene and supergene alunite based on progressive heating experiments from 100 to 1000 degrees C. *Geochim Cosmochim Acta* 60:4525-4535
- Kelley SP (1988) The relationship between K-Ar mineral ages, mica grain sizes and movement on the Moine Thrust Zone, NW Highlands, Scotland. *J Geol Soc London* 145:1-10
- Kelley SP (2002) Excess Argon in K-Ar and Ar-Ar Geochronology. *Chem Geol* (in press)
- Kelley SP, and Bluck BJ (1989) Detrital mineral ages from the Southern Uplands using $^{40}\text{Ar}/^{39}\text{Ar}$ laser probe. *J Geol Soc London*, 146:401-403
- Kelley SP, Turner G (1991) Laser probe $^{40}\text{Ar}-^{39}\text{Ar}$ measurements of loss profiles within individual hornblende grains from the Giants Range Granite, northern Minnesota, USA. *Earth Planet Sci Lett* 107:634-648
- Kelley SP, Wartho J-A (2000) Rapid kimberlite ascent and the significance of Ar-Ar ages in xenolith phlogopites. *Science* 289:609-611
- Kelley SP, Turner G, Butterfield AW, Shepherd TJ (1986) The source and significance of argon in fluid inclusions from areas of mineralization. *Earth Planet Sci Lett* 79:303-318
- Kelley SP, Reddy SM, Maddock R (1994) $^{40}\text{Ar}/^{39}\text{Ar}$ laser probe investigation of a pseudotachylyte vein from the Moine Thrust Zone, Scotland. *Geology* 22:443-446
- Kelley SP, Bartlett JM, Harris NBW (1997) Pre-metamorphic ages from biotite inclusions in garnet. *Geochim Cosmochim Acta* 61:3873-3878
- Kendrick MA, Burgess R, Patrick RAD, Turner G (2001a) Fluid inclusion noble gas and halogen evidence on the origin of Cu-porphyry mineralizing fluids. *Geochim Cosmochim Acta* 65:2651-2668
- Kendrick MA, Burgess R, Patrick RAD, Turner PG (2001b) Halogen and Ar-Ar age determinations of inclusions within quartz veins from porphyry copper deposits using complementary noble gas extraction techniques. *Chem Geol* 177:351-370
- Kipfer R, Aeschbach-Hertig W, Peeters F, Stute M (2002) Noble gases in lakes and groundwaters. *Rev Mineral Geochem* 47:615-700
- Kirschner DL, Cosca MA, Masson H, Hunziker JC (1996) Staircase Ar-40/Ar-39 spectra of fine-grained-white mica: Timing and duration of deformation and empirical constraints on argon diffusion. *Geology* 24:747-750
- Kramar N, Cosca MA, Hunziker JC (2001) Heterogeneous Ar-40* distributions in naturally deformed muscovite: *In situ* UV-laser ablation evidence for micro structurally controlled intra-grain diffusion. *Earth Planet Sci Lett* 192:377-388

- Lanphere MA, Dalrymple GB (1976) Identification of Excess ^{40}Ar by the $^{40}\text{Ar}/^{39}\text{Ar}$ age spectrum technique. *Earth Planet Sci Lett* 32:141-148
- Lanphere MA, Baadsgaard H (2001) Precise K-Ar, ^{40}Ar - ^{39}Ar , Rb-Sr and U/Pb mineral ages from the 27.5 Ma Fish Canyon Tuff reference standard. *Chem Geol* 175:653-671
- Layer PW, Kroner A, McWilliams M, York D (1989) Elements of the Archean thermal history and apparent polar wander of the Eastern Kaapvaal Craton, Swaziland, from single grain dating and paleomagnetism. *Earth Planet Sci Lett* 93:23-34
- Lee JKW (1993) The argon release mechanisms of hornblende *in vacuo*. *Chem Geol (Isotop Geosci Sect)* 106:133-170
- Lee JKW (1995) Multipath diffusion in geochronology. *Contrib Mineral Petrol* 120:60-82
- Lee JKW, Onstott TC, Hanes JA (1990) An $^{40}\text{Ar}/^{39}\text{Ar}$ investigation of the contact effects of a dyke intrusion, Kapuskasing Structural Zone, Ontario: A comparison of laser microprobe and furnace extraction techniques. *Contrib Mineral Petrol* 105:87-105
- Lee JKW, Onstott TC, Cashman KV, Cumbest RJ, Johnson D (1991) Incremental heating of hornblende *in vacuo*: Implications for $^{40}\text{Ar}/^{39}\text{Ar}$ geochronology and the interpretation of thermal histories. *Geology* 19:872-876
- Li S, Wang S, Chen Y, Liu D, Qiu J, Zhou H, Zhang Z (1994) Excess argon in phengite from eclogite: evidence from dating of eclogite minerals by Sm-Nd, Rb-Sr and $^{40}\text{Ar}/^{39}\text{Ar}$ methods. *Chem Geol (Isotop Geosci Sect)* 112:343-350
- Lister GS, Baldwin SL (1996) Modeling the effect of arbitrary P-T-t histories on argon diffusion in minerals using the MacArgon program for the Apple Macintosh. *Tectonophysics* 253:83-109
- Livingston DE, Damon PE, Mauger RL, Bennet R, Laughlin AW (1967) Argon-40 in cogenetic feldspar-mica mineral assemblages. *J Geophys Res* 72:1361-1375
- Lo C-H, Onstott TC (1989) ^{39}Ar recoil artifacts in chloritized biotite. *Geochim Cosmochim Acta* 53:2697-2711
- Lo CH, Lee JKW, Onstott TC (2000) Argon release mechanisms of biotite *in vacuo* and the role of short-circuit diffusion and recoil. *Chem Geol* 165:135-166
- Lovera OM, Richter FM, Harrison TM (1989) The $^{40}\text{Ar}/^{39}\text{Ar}$ thermochronometry for slowly cooled samples having a distribution of diffusion domain sizes. *J Geophys Res* 94:917-935
- Lovera OM, Richter FM, Harrison TM (1991) Diffusion domains determined by ^{39}Ar released during step heating. *J Geophys Res* 96:2057-2069
- Lovera OM, Heizler MT, Harrison TM (1993) Argon diffusion domains in K-feldspar, II: Kinetic parameters of MH-10. *Contrib Mineral Petrol* 113:381-393
- Lovera OM, Grove M, Harrison TM, Mahon KI (1997) Systematic analysis of K-feldspar $^{40}\text{Ar}/^{39}\text{Ar}$ step heating results: I. Significance of activation energy determinations. *Geochim Cosmochim Acta* 61:3171-3192
- Lovering JF, Richards JR (1964) Potassium-argon age study of possible lower-crust and upper-mantle inclusions in deep-seated intrusions. *J Geophys Res* 69:4895-4901
- Ludwig KR, Renne PR (2000) Geochronology on the paleoanthropological time scale. *Evol Anthropol* 9:101-110
- Magloughlin JF, Hall CM, van der Pluijm BA (2001) Ar-40-Ar-39 geochronometry of pseudotachylytes by vacuum encapsulation: North Cascade Mountains, Washington, USA. *Geology* 29:51-54
- Mahon KI, Harrison TM, Grove M (1998) The thermal and cementation histories of a sandstone petroleum reservoir, Elk Hills, California. *Chem Geol* 152:227-256
- Marshall BD, DePaolo DJ (1982) Precise age determinations and petrogenetic studies using the K-Ca method. *46:2537-2545*
- McDougall I, Harrison TM. (1999) *Geochronology and Thermochronology by the $^{40}\text{Ar}/^{39}\text{Ar}$ method*. Oxford University Press, New York, 212 p
- Merrihue CM (1965) Trace-element determinations and potassium-argon dating by mass spectroscopy of neutron irradiated samples. *EOS Trans Am Geophys Union* 46:125 (abstr)
- Merrihue CM, Turner G (1966) Potassium-argon dating by activation with fast neutrons. *J Geophys Res* 71:2852-2857
- Min K, Mundil R, Renne PR, Ludwig KR (2000) A test for systematic errors in ^{40}Ar - ^{39}Ar geochronology through comparison with U-Pb analysis of a 1.1 Ga rhyolite. *Geochim Cosmochim Acta* 64:73-98
- Min K, Farley KA, Renne P (2001) Single-grain (U-Th)/He Ages from apatites in Acapulco meteorite. *EOS Trans Am Geophys Union Fall Mtg 2001 Suppl Abstr* V22C-1059
- Mitchell JG (1968) The argon-40/argon-39 method of potassium-argon age determination. *Geochim Cosmochim Acta* 32:781-790
- Mock C, Arnaud NO, Cantagrel JM (1999a) An early unroofing in northeastern Tibet? Constraints from Ar-40/Ar-39 thermochronology on granitoids from the eastern Kunlun range (Qianghai, NW China). *Earth Planet Sci Lett* 171:107-122

- Mock C, Arnaud NO, Cantagrel JM, Yirgu G (1999b) Ar-40/Ar-39 thermochronology of the Ethiopian and Yemeni basements: reheating related to the Afar plume? *Tectonophysics* 314:351-372
- Mulch A, Cosca MA, Handy MR (2002) *In situ* UV-laser $^{40}\text{Ar}/^{39}\text{Ar}$ geochronology of a micaceous mylonite: an example of defect-enhanced argon loss. *Contrib Mineral Petrol* 142:738-752
- Muller W, Prosser G, Mancktelow NS, Villa IM, Kelley SP, Viola G, Oberli F (2001) Geochronological constraints on the evolution of the Periadriatic Fault System (Alps). *Intl J Earth Sci* 90:623-653
- Niedermann S (2002) Cosmic-ray-produced noble gases in terrestrial rocks as a dating tool for surface processes. *Rev Mineral Geochem* 47:731-784
- Nier AO (1950) A redetermination of the relative abundances of the isotopes of carbon, nitrogen, oxygen, argon and potassium. *Phys Rev* 77:789-793
- Oberli F, Fischer H, Meier M (1990) High-resolution ^{238}U - ^{206}Pb zircon dating of Tertiary bentonites and the Fish Canyon Tuff: a test for age "concordance" by single-crystal analysis. *Geol Soc Australia* 27:74 (abstr)
- Onstott TC, Peacock MW (1987) Argon retentivity of hornblendes: A field experiment in a slowly cooled metamorphic terrane. *Geochim Cosmochim Acta* 51:2891-2903
- Onstott TC, Phillips D, Pringle-Goodell L (1991) Laser Microprobe Measurement of Chlorine and Argon Zonation in Biotite. *Chem Geol* 90:145-168
- Onstott TC, Miller ML, Ewing RC, Arnold GW, Walsh DS (1995) Recoil refinements: Implications for the $^{40}\text{Ar}/^{39}\text{Ar}$ dating technique. *Geochim Cosmochim Acta* 59:1821-1834
- Onstott TC, Mueller C, Vrolijk PJ, Pevear DR (1997) Laser Ar-40/Ar-39 microprobe analyses of fine-grained illite. *Geochim Cosmochim Acta* 61:3851-3861
- Pankhurst RJ, Moorbath S, Rex DC, Turner G (1973) Mineral age patterns in ca. 3700 m.y. old rocks from West Greenland. *Earth Planet Sci Lett* 20:157-170
- Parsons I, Brown WL, Smith JV (1999) $^{40}\text{Ar}/^{39}\text{Ar}$ thermochronology using alkali feldspars: Real thermal history or mathematical mirage of microtexture? *Contrib Mineral Petrol* 136:92-110.
- Pearson RC, Hedge CE, Thomas HH, Stearn TW (1966) Geochronology of the St Kevin Granite and neighboring Precambrian rocks, northern Sawatch Range, Colorado. *Geol Soc Am Bull* 77:1109-1120
- Philippot P, Rumble D (2000) Fluid-rock interactions during high-pressure and ultrahigh-pressure metamorphism. *Intl Geol Rev* 42:312-327
- Phillips D, Onstott TC (1988) Argon isotopic zoning in mantle phlogopite. *Geology* 16:542-546
- Pickles CS, Kelley SP, Reddy SM, Wheeler J (1997) Determination of high spatial resolution argon isotope variations in metamorphic biotites. *Geochim Cosmochim Acta* 61:3809-3883
- Polyak VJ, McIntosh WC, Guven N, Provencio P (1998) Age and origin of Carlsbad cavern and related caves from Ar-40/Ar-39 of alunite. *Science* 279:1919-1922
- Pringle MS, Staudigel H, Gee J (1991) Jasper Seamount—7 million years of volcanism. *Geology* 19:364-368
- Purdy JW, Jäger E. (1976) K-Ar ages on rock-forming minerals from the Central Alps. *Mem Geol Inst Univ Padova* 30, 31 p
- Rama SNI, Hart SR, Roedder E (1965) Excess radiogenic argon in fluid inclusions. *J Geophys Res* 70:509-511
- Reddy SM, Kelley SP, Wheeler J (1996) A $^{40}\text{Ar}/^{39}\text{Ar}$ laser probe study of micas from the Sesia Zone, Italian Alps: Implications for metamorphic and deformation histories. *J Metamorph Geol* 14:493-508
- Reddy SM, Kelley SP, Magennis L (1997) A microstructural and argon laserprobe study of shear zone development at the western margin of the Nanga Parbat-Haramosh Massif, western Himalaya. *Contrib Mineral Petrol* 128:16-29
- Reddy SM, Potts GJ, Kelley SP (2001) $^{40}\text{Ar}/^{39}\text{Ar}$ ages in deformed potassium feldspar: Evidence of microstructural control on Ar isotope systematics. *Contrib Mineral Petrol* 141:186-200
- Renne PR (1995) Excess ^{40}Ar in biotite and hornblende from the Norilsk-1 Intrusion, Siberia—Implications for the age of the Siberian Traps. *Earth Planet Sci Lett* 134:225-225
- Renne PR (2000) Ar-40/Ar-39 age of plagioclase from Acapulco meteorite and the problem of systematic errors in cosmochronology. *Earth Planet Sci Lett* 175:13-26
- Renne PR (2001) Reply to Comment on "Ar-40/Ar-39 age of plagioclase from Acapulco meteorite and the problem of systematic errors in cosmochronology" by Mario Trieloff, Elmar K. Jessberger and Christine Fieni. *Earth Planet Sci Lett* 190:271-273
- Renne PR, Basu AR (1991) Rapid eruption of the Siberian Traps flood basalts at the Permo-Triassic boundary. *Science* 253:176-179
- Renne PR, Norman EB (2001) Determination of the half-life of Ar-37 by mass spectrometry. *Phys Rev C* 6304:7302
- Renne PR, Ernesto M, Pacca IG, Coe RS, Glen JM, Prevot M, Perrin M (1992) The age of Parana flood volcanism, rifting of Gondwanaland, and the Jurassic-Cretaceous boundary. *Science* 258:975-979

- Renne PR, Deino AL, Walter RC, Turrin BD, Swisher CC, Becker TA, Curtis GH, Sharp WD, Jaoui AR (1994) Intercalibration of astronomical and radioisotopic time. *Geology* 22:783-786
- Renne PR, Zhang ZC, Richards MA, Black MT, Basu AR (1995) Synchrony and causal relations between Permian-Triassic boundary crises and Siberian flood volcanism. *Science* 269:1413-1416
- Renne PR, Glen JM, Milner SC, Duncan AR (1996a) Age of Etendeka flood volcanism and associated intrusions in southwestern Africa. *Geology* 24:659-662
- Renne PR, Deckart K, Ernesto M, Feraud G, Piccirillo EM (1996b) Age of the Ponta Grossa dike swarm (Brazil), and implications to Parana flood volcanism. *Earth Planet Sci Lett* 144:199-211
- Renne PR, Sharp WD, Deino AL, Orsi G, Civetta L (1997) Ar-40/Ar-39 dating into the historical realm: Calibration against Pliny the Younger. *Science* 277:1279-1280
- Renne PR, Karner DB, Ludwig KR (1998a) Radioisotope dating—Absolute ages aren't exactly. *Science* 282:1840-1841
- Renne PR, Swisher CC, Deino AL, Karner DB, Owens TL, DePaolo DJ (1998b) Inter-calibration of standards, absolute ages and uncertainties in $^{40}\text{Ar}/^{39}\text{Ar}$ dating. *Chem Geol* 145:117-152
- Renne PR, Farley KA, Becker TA, Sharp WD (2001) Terrestrial cosmogenic argon. *Earth Planet Sci Lett* 188:435-440
- Roddick JC (1978) The application of isochron diagrams in $^{40}\text{Ar}/^{39}\text{Ar}$ dating: A discussion. *Earth Planet Sci Lett* 41:233-244
- Roddick JC, Cliff RA, Rex DC (1980) The evolution of excess argon in Alpine biotites—A $^{40}\text{Ar}-^{39}\text{Ar}$ analysis. *Earth Planet Sci Lett* 48:185-208
- Roselieb K, Wartho J-A, Buttner H, Jambon A, Kelley SP (1999) Solubility and diffusivity of noble gases in synthetic phlogopite: A UV LAMP investigation. 4:368
- Ruffet G, Gruau G, Ballèvre M, Féraud G, Philipot P (1997) Rb-Sr and $^{40}\text{Ar}-^{39}\text{Ar}$ laser probe dating of high-pressure phengites from the Sesia Zone (Western Alps): Underscoring of excess argon and new age constraints on high-pressure metamorphism. *Chem Geol* 141:1-18
- Samson SD, Alexander EC (1987) Calibration of the interlaboratory $^{40}\text{Ar}-^{39}\text{Ar}$ dating standard—MMhb-1. *Chem Geol (Isotop Geosci Sect)* 66:27-34
- Scailliet S (1996) Excess ^{40}Ar transport scale and mechanism in high-pressure phengites: A case study from an eclogitized metabasite of the Dora-Maira nappe, western Alps. *Geochim Cosmochim Acta* 60:1075-1090
- Scailliet S (2000) Numerical Error Analysis in Ar-40/Ar-39 Dating. *Chem Geol* 162:269-298
- Scailliet S, Feraud G, Lagabrielle Y, Balleve M, Ruffet G (1990) Ar-40/Ar-39 laser-probe dating by step heating and spot fusion of phengites from the Dora-Maira nappe of the Western Alps, Italy. *Geology* 18:741-744
- Scailliet S, Féraud G, Ballèvre M, Amouric M (1992) Mg/Fe and [(Mg,Fe)Si-Al₂] compositional control on argon behavior in high-pressure white micas: A $^{40}\text{Ar}/^{39}\text{Ar}$ continuous laser-probe study from the Dora-Maira nappe of the internal western Alps, Italy. *Geochim Cosmochim Acta* 56:2851-2872
- Schaeffer OA, Zähringer J. (1966) Potassium Argon Dating. Springer-Verlag, New York, 234 p
- Schmitz MD, Bowring SA (2001) U-Pb zircon and titanite systematics of the Fish Canyon Tuff: an assessment of high-precision U-Pb geochronology and its application to young volcanic rocks. *Geochim Cosmochim Acta* 65:2571-2587
- Sherlock SC (2001) Two-stage erosion and deposition in a continental margin setting: a $^{40}\text{Ar}/^{39}\text{Ar}$ laserprobe study of offshore detrital white micas in the Norwegian Sea. *J Geol Soc London* 158:793-800
- Sherlock SC, Arnaud NO (1999) Flat plateau and impossible isochrons: Apparent $^{40}\text{Ar}-^{39}\text{Ar}$ geochronology in a high-pressure terrain. *Geochim Cosmochim Acta* 63:2835-2838
- Sherlock SC and Kelley SP (2002) Excess argon evolution in HP-LT rocks: A UVLAMP study of phengite and K-free minerals, NW Turkey. *Chem Geol* (in press)
- Sherlock SC, Kelley SP, Inger S, Harris NBW, Okay A (1999) $^{40}\text{Ar}-^{39}\text{Ar}$ and Rb-Sr geochronology of high-pressure metamorphism and exhumation history of the Tavsanli Zone, NW Turkey. *Contrib Mineral Petrol* 137:46-58
- Singer B, Hildreth W, Vincze Y (2000) Ar-40/Ar-39 evidence for early deglaciation of the central Chilean Andes. *Geophys Res Lett* 27:1663-1666
- Singer BS, Pringle MS (1996) Age and duration of the Matuyama-Brunhes geomagnetic polarity reversal from Ar-40/Ar-39 incremental heating analyses of lavas. *Earth Planet Sci Lett* 139:47-61
- Smith PE, Evensen NM, York D (1993) First successful $^{40}\text{Ar}-^{39}\text{Ar}$ dating of glauconites: Argon recoil in single grains of cryptocrystalline material. *Geology* 21:41-44
- Smith PE, York D, Easton RM, Özdemir Ö, Layer PW (1994) A laser $^{40}\text{Ar}/^{39}\text{Ar}$ study of minerals across the Grenville Front: Investigations of reproducible excess Ar patterns. *Can J Earth Sci* 31:808-817
- Smith SP, Kennedy BM (1983) The Solubility of noble gases in water and in NaCl brine. *Geochim Cosmochim Acta* 47:503-515

- Smits F, Gentner W (1950) Argonbestimmungen an Kalium-Mineralien I. Bestimmungen an tertiären Kalisalzen. *Geochim Cosmochim Acta* 1:22-27
- Spray JG, Kelley SP, Reimold WU (1995) Laser probe argon⁴⁰/argon³⁹ dating of coesite- and stishovite-bearing pseudotachylytes and the age of the Vredefort impact event. *Meteoritics* 30:335-343
- Steiger RJ, Jäger E (1977) Subcommittee on geochronology: Convention on the use of decay constants in geo- and cosmochronology. *Earth Planet Sci Lett* 36:359-362
- Storey M, Mahoney JJ, Saunders AD, Duncan RA, Kelley SP, Coffin MF (1995) Timing of hot spot-related volcanism and the breakup of Madagascar and India. *Science* 267:852-855
- Swindle TD (2002) Noble gases in the moon and meteorites—Radiogenic components and early volatile chronologies. *Rev Mineral Geochem* 47:101-124
- Ton-That T, Singer B, Paterne M (2001) Ar-40/Ar-39 dating of latest Pleistocene (41 Ka) marine tephra in the Mediterranean Sea: implications for global climate records. *Earth Planet Sci Lett* 184:645-658
- Torgersen T, B.M. K, Hiagon H, Chiou KY, J.H. R, Clarke WB (1989) Argon accumulation and the crustal degassing flux of ⁴⁰Ar in the Great Atresian Basin, Australia. *Earth Planet Sci Lett* 92:43-56
- Trieloff M, Jessberger EK, Fieni C (2001) Comment on “Ar-40/Ar-39 age of plagioclase from Acapulco meteorite and the problem of systematic errors in cosmochronology” by Paul R. Renne. *Earth Planet Sci Lett* 190:263-265
- Turner G (1969) Thermal histories of meteorites by the 39Ar-40Ar method. In Millman PM (ed) *Meteorite Research*. D. Reidel Publishing, Dordrecht, The Netherlands, p 407-417
- Turner G (1970a) Thermal histories of meteorites. In Runcorn SK (ed) *Paleogeophysics*. Academic Press, London, p 491-502
- Turner G (1970b) ⁴⁰Ar-³⁹Ar age determination of lunar rock 12013. *Earth Planet Sci Lett* 9:177-180
- Turner G (1970c) Argon-40/argon-39 dating of lunar rock samples. *Science* 167:466-468
- Turner G (1971a) ⁴⁰Ar-³⁹Ar dating: The optimization of irradiation parameters. *Earth Planet Sci Lett* 10:227-234
- Turner G (1971b) ⁴⁰Ar-³⁹Ar ages from the lunar maria. *Earth Planet Sci Lett* 11:169-191
- Turner G (1972) ⁴⁰Ar-³⁹Ar age and cosmic ray irradiation history of the Apollo 15 anorthosite 15415. *Earth Planet Sci Lett* 14:169-175
- Turner G (1977) Potassium-argon chronology of the moon. *Phys Chem Earth* 10:145-195
- Turner G, Cadogan PH (1974) Possible effects of ³⁹Ar recoil in ⁴⁰Ar-³⁹Ar dating. *Geochim Cosmochim Acta* 5:1601-1615
- Turner G, Bannon MP (1992) Argon isotope geochemistry of inclusion fluids from granite-associated mineral veins in southwest and northeast England. *Geochim Cosmochim Acta* 56:227-243
- Turner G, Wang S (1992) Excess argon, crustal fluids and apparent isochrons from crushing K-feldspar. *Earth Planet Sci Lett* 110:193-211
- Turner G, Burnard P, Ford JL, Gilmour JD, Lyon IC, Stuart FM (1993) Tracing fluid sources and interactions. *Phil Trans Roy Soc London Ser A* 344:127-140
- Turner G, Knott SF, Ash RD, Gilmour JD (1997) Ar-Ar chronology of the Martian meteorite ALH84001: Evidence for the timing of the early bombardment of Mars. *Geochim Cosmochim Acta* 61:3835-3850
- van der Bogaard P, Schirnack C (1995) ⁴⁰Ar/³⁹Ar laser-probe ages of Bishop Tuff quartz phenocrysts substantiate long-lived silicic magma chamber at Long Valley, United States. *Geology* 23:759-762
- Vance D, Ayres M, Kelley SP, Harris NBW (1998) The thermal response of a metamorphic belt to extension: constraints from laser Ar data on metamorphic micas. *Earth Planet Sci Lett* 162:153-164
- Vasconcelos PM (1999) K-Ar and Ar-40/Ar-39 geochronology of weathering processes. *Ann Rev Earth Planet Sci* 27:183-229
- Villa IM (1994) Multipath Ar transport in K-feldspar deduced from isothermal heating experiments. *Earth Planet Sci Lett* 122:393-401
- Villa IM (1997) Direct determination of ³⁹Ar recoil distance. *Geochim Cosmochim Acta* 61:689-691
- Villa IM, Grobety B, Kelley SP, Trigila R, Wieler R (1996) Assessing Ar transport paths and mechanisms in the McClure Mountains hornblende. *Contrib Mineral Petrol* 126:67-80
- Warnock AC, Zeitler PK (1998) Ar-40/Ar-39 thermochronometry of K-feldspar from the KTB borehole, Germany. *Earth Planet Sci Lett* 158:67-79
- Wartho JA (1995) Apparent Argon Diffusive Loss Ar-40/Ar-39 Age Spectra in Amphiboles. *Earth Planet Sci Lett* 134:393-407
- Wartho JA, Dodson MH, Rex DC, Guise PG (1991) Mechanisms of Ar release from Himalayan metamorphic hornblende. *Am Mineral* 76:1446-1448
- Wartho J-A, Rex DD, Guise PG (1996) Excess argon in amphiboles linked to greenschist facies alteration in Kamila amphibolite belt, Kohistan island arc system, northern Pakistan: Insights from ⁴⁰Ar/³⁹Ar step-heating and acid leaching experiments. *Geol Mag* 133:595-609

- Wartho JA, Kelley SP, Brooker RA, Carroll MR, Villa IM, Lee MR (1999) Direct measurement of Ar diffusion profiles in a gem-duality Madagascar K-feldspar using the ultra-violet laser ablation microprobe (UVLAMP). *Earth Planet Sci Lett* 170:141-153
- Wartho JA, Kelley SP, Blake S (2001) Magma flow regimes in sills deduced from Ar isotope systematics of host rocks. *J Geophys Res-Solid Earth* 106:4017-4035
- Wieler R (2002) Cosmic-ray-produced noble gases in meteorites. *Rev Mineral Geochem* 47:125-170
- Wheeler J (1996) A program for simulating argon diffusion profiles in minerals. *Computers Geosciences* 28:919-929
- Wilch TI, McIntosh WC, Dunbar NW (1999) Late Quaternary volcanic activity in Marie Byrd Land: Potential Ar-40/Ar-39-dated time horizons in West Antarctic ice and marine cores. *Geol Soc Am Bull* 111:1563-1580
- Wright N, Layer PW, York D (1991) New insights into thermal history from single grain Ar-40/Ar-39 analysis of biotite. *Earth Planet Sci Lett* 104:70-79
- Zeitler PK, FitzGerald JD (1986) Saddle-shaped $^{40}\text{Ar}/^{39}\text{Ar}$ age spectra from young, microstructurally complex potassium feldspars. *Geochim Cosmochim Acta* 50:1185-1199